

# Theoretical Implications of the PSR B1620–26 Triple System and its Planet

Eric B. Ford<sup>1</sup>, Kriten J. Joshi<sup>2</sup>, Frederic A. Rasio<sup>3,4</sup> and Boris Zbarsky<sup>5</sup>

Department of Physics, Massachusetts Institute of Technology

## ABSTRACT

We present a new theoretical analysis of the PSR B1620–26 triple system in the globular cluster M4, based on the latest radio pulsar timing data, which now include measurements of five time derivatives of the pulse frequency. These data allow us to determine the mass and orbital parameters of the second companion completely (up to the usual unknown orbital inclination angle  $i_2$ ). The current best-fit parameters correspond to a second companion of planetary mass,  $m_2 \sin i_2 \simeq 7 \times 10^{-3} M_\odot$ , in an orbit of eccentricity  $e_2 \simeq 0.45$  and semimajor axis  $a_2 \simeq 60$  AU. Using numerical scattering experiments, we study a possible formation scenario for the triple system, which involves a dynamical exchange interaction between the binary pulsar and a primordial star–planet system. The current orbital parameters of the triple are consistent with such a dynamical origin, and suggest that the separation of the parent star–planet system was very large,  $\gtrsim 50$  AU. We also examine the possible origin of the anomalously high eccentricity of the inner binary pulsar. While this eccentricity could have been induced during the same dynamical interaction that created the triple, we find that it could equally well arise from long-term secular perturbation effects in the triple, combining the general relativistic precession of the inner orbit with the Newtonian gravitational perturbation of the planet. The detection of a planet in this system may be taken as evidence that large numbers of extrasolar planetary systems, not unlike those discovered recently in the solar neighborhood, also exist in old star clusters.

*Subject headings:* binaries: wide — celestial mechanics, stellar dynamics — planetary systems — pulsars: general — pulsars: individual (PSR B1620–26)

---

<sup>1</sup>6-218M MIT, 77 Massachusetts Ave, Cambridge, MA 02139; email: eford@mit.edu.

<sup>2</sup>6-218M MIT, 77 Massachusetts Ave, Cambridge, MA 02139; email: kjoshi@mit.edu.

<sup>3</sup>6-201 MIT, 77 Massachusetts Ave, Cambridge, MA 02139; email: rasio@mit.edu.

<sup>4</sup>Alfred P. Sloan Research Fellow.

<sup>5</sup>6-218M MIT, 77 Massachusetts Ave, Cambridge, MA 02139; email: bzbarsky@mit.edu.

## 1. Introduction

PSR B1620–26 is a unique millisecond radio pulsar. The pulsar is a member of a hierarchical triple system located in or near the core of the globular cluster M4. It is the only radio pulsar known in a triple system, and the only triple system known in any globular cluster. The inner binary of the triple contains the  $\simeq 1.4 M_{\odot}$  neutron star with a  $\simeq 0.3 M_{\odot}$  white-dwarf companion in a 191-day orbit (Lyne *et al.* 1988; McKenna & Lyne 1988) The triple nature of the system was first proposed by Backer (1993) in order to explain the unusually high residual second and third pulse frequency derivatives left over after subtracting a standard Keplerian model for the pulsar binary.

The pulsar has now been timed for eleven years since its discovery (Thorsett, Arzoumanian, & Taylor 1993; Backer, Foster, & Sallmen 1993; Backer & Thorsett 1995; Arzoumanian *et al.* 1996; Thorsett *et al.* 1999). These observations have not only confirmed the triple nature of the system, but they have also provided tight constraints on the mass and orbital parameters of the second companion. Earlier calculations using three pulse frequency derivatives suggested that the mass of the second companion could be anywhere between  $10^{-3}$  and  $1 M_{\odot}$ , with corresponding orbital periods in the range  $\sim 10^2 - 10^3$  yr (Michel 1994; Rasio 1994; Sigurdsson 1995). More recent calculations using four frequency derivatives and preliminary measurements of the orbital perturbations of the inner binary have further constrained the mass of the second companion, and strongly suggest that it is a giant planet or a brown dwarf of mass  $\sim 0.01 M_{\odot}$  at a distance  $\sim 50$  AU from the pulsar binary (Arzoumanian *et al.* 1996; Joshi & Rasio 1997). In this paper we present a new analysis of the pulsar timing data, including the most recent observations of Thorsett *et al.* (1999; hereafter TACL). The data now include measurements of five pulse frequency derivatives, as well as improved measurements and constraints on various orbital perturbation effects in the triple.

Previous optical observations by Bailyn *et al.* (1994) and Shearer *et al.* (1996) using ground-based images of M4 had identified a possible optical counterpart for the pulsar, consistent with a  $\sim 0.5 M_{\odot}$  main-sequence star, thus contradicting the theoretical results, which suggest a much lower-mass companion. However, it also seemed possible that the object could be a blend of unresolved fainter stars, if not a chance superpositon. Later HST WFPC2 observations of the same region by Bailyn *et al.* (1999) have resolved the uncertainty. The much higher resolution ( $\sim 0.1''$ ) HST image shows no optical counterpart at the pulsar position, down to a magnitude of  $V \simeq 23$ , therefore eliminating the presence of any main-sequence star in the system. Thus, the optical observations are now consistent with the theoretical modeling of the pulsar timing data.

PSR B1620–26 is not the first millisecond pulsar system in which a planet (or brown dwarf) has been detected. The first one, PSR B1257+12, is an isolated millisecond pulsar with three clearly detected inner planets (all within 1 AU) of terrestrial masses in circular orbits around the neutron star (Wolszczan 1994). Preliminary evidence for at least one giant planet orbiting at a much larger distance from the neutron star has also been reported (Wolszczan 1996; see the

theoretical analysis in Joshi & Rasio 1997). In PSR B1257+12 it is likely that the planets were formed in orbit around the neutron star, perhaps out of a disk of debris left behind following the complete evaporation of the pulsar’s stellar binary companion (see, e.g., Podsiadlowski 1995). Such an evaporation process has been observed in several eclipsing binary millisecond pulsars, such as PSR B1957+20 (Arzoumanian *et al.* 1994) and PSR J2051-0827 (Stappers *et al.* 1996), where the companion masses have been reduced to  $\sim 0.01 - 0.1 M_{\odot}$  by ablation. These companions used to be ordinary white dwarfs and, although their masses are now quite low, they cannot be properly called either planets or brown dwarfs.

In PSR B1620–26, the hierarchical triple configuration of the system and its location near the core of a dense globular cluster suggest that the second companion was acquired by the pulsar following a dynamical interaction with another object (Rasio, McMillan & Hut 1995; Sigurdsson 1995). This object could have been a primordial binary with a low-mass brown-dwarf component, or a main-sequence star with a planetary system containing at least one massive giant planet. Indeed the possibility of detecting “scavenged” planets around millisecond pulsars in globular clusters was discussed by Sigurdsson (1992) even before the triple nature of PSR B1620–26 was discovered.

Objects with masses  $\sim 0.001 - 0.01 M_{\odot}$  have recently been detected around many nearby solar-like stars in Doppler searches for extrasolar planets (see Marcy & Butler 1998 for a review). In at least one case, Upsilon Andromedae, several objects have been detected in the same system, clearly establishing that they are members of a planetary system rather than a very low-mass stellar (brown dwarf) binary companion (Butler *et al.* 1999). For the second companion of PSR B1620–26, of mass  $\sim 0.01 M_{\odot}$ , current observations and theoretical modeling do not make it possible to determine whether the object was originally formed as part of a planetary system, or as a brown dwarf. In this paper, we will simply follow our prejudice, and henceforth will refer to the object as “the planet.”

One aspect of the system that remains unexplained, and can perhaps provide constraints on its formation and dynamical evolution, is the unusually high eccentricity  $e_1 = 0.0253$  of the inner binary. This is much larger than one would expect for a binary millisecond pulsar formed through the standard process of pulsar recycling through accretion from a red giant companion. During the mass accretion phase, tidal circularization of the orbit through turbulent viscous dissipation in the red-giant envelope should have brought the eccentricity down to  $\lesssim 10^{-4}$  (Phinney 1992). At the same time, however, the measured value may appear too small for a dynamically induced eccentricity. Indeed, for an initially circular binary, the eccentricity induced by a dynamical interaction with another star is an extremely steep function of the distance of closest approach (Rasio & Heggie 1995). Therefore a “typical” interaction would be expected either to leave the eccentricity unchanged, or to increase it to a value of order unity (including the possibility of disrupting the binary). In addition, one expects that most “exchange” interactions with a star–planet system will lead to the ejection of the planet while the star is retained in a bound orbit around the pulsar binary (Rasio *et al.* 1995; Heggie, Hut, & McMillan 1996). In this paper

we will present the results of new numerical scattering experiments simulating encounters between the binary pulsar and a star–planet system. These simulations allow us to estimate quantitatively the probability of retaining the planet in the triple, while perhaps at the same time inducing a small but significant eccentricity in the pulsar binary.

Secular perturbations in the triple system can also lead to an increase in the eccentricity of the inner binary. A previous analysis assuming nearly coplanar orbits suggested that, starting from a circular inner orbit, an eccentricity as large as 0.025 could only be induced by the perturbation from a stellar-mass second companion (Rasio 1994), which is now ruled out. For large relative inclinations, however, it is known that the eccentricity perturbations can in principle be considerably larger (Kozai 1962; see Ford, Kozinsky & Rasio 1999 for a recent treatment). In addition, the Newtonian secular perturbations due to the tidal field of the second companion can combine nonlinearly with other perturbation effects, such as the general relativistic precession of the inner orbit, to produce enhanced eccentricity perturbations (Ford *et al.* 1999). In this paper, we re-examine the effects of secular perturbations on eccentricity in the PSR B1620–26 triple, taking into account the possibly large relative inclination of the orbits, as well as the interaction between Newtonian perturbations and the general relativistic precession of the pulsar binary.

## 2. Analysis of the Pulsar Timing Data

### 2.1. Pulse Frequency Derivatives

The standard method of fitting a Keplerian orbit to timing residuals cannot be used when the pulsar timing data cover only a small fraction of the orbital period (but see TACL for an attempt at fitting two Keplerian orbits to the PSR B1620–26 timing data). For PSR B1620–26, the duration of the observations, about 11 years, is very short compared to the likely orbital period of the second companion,  $\gtrsim 100$  yr. In this case, pulse frequency derivatives (coefficients in a Taylor expansion of the pulse frequency around a reference epoch) can be derived to characterize the shape of the timing residuals (after subtraction of a Keplerian model for the inner binary). It is easy to show that from *five* well-measured and dynamically-induced frequency derivatives one can obtain a complete solution for the orbital parameters and mass of the companion, up to the usual inclination factor (Joshi & Rasio 1997; hereafter JR97).

In our previous analysis of the PSR B1620–26 system (JR97), we used the first four time derivatives of the pulse frequency to solve for a one-parameter family of solutions for the orbital parameters and mass of the second companion. The detection of the fourth derivative, which was marginal at the time, has now been confirmed (TACL). In addition, we now also have a preliminary measurement of the *fifth* pulse derivative. This allows us in principle to obtain a unique solution, but the measurement uncertainty on the fifth derivative is very large, giving us correspondingly large uncertainties on the theoretically derived parameters of the system. Equations and details on the method of solution were presented in JR97, and will not be repeated here.

Our new solution is based on the latest available values of the pulse frequency derivatives, obtained by TACL for the epoch MJD 2448725.5:

$$\begin{aligned}
 \text{Spin Period } P &= 11.0757509142025(18) \text{ ms} \\
 \text{Spin frequency } f &= 90.287332005426(14) \text{ s}^{-1} \\
 \dot{f} &= -5.4693(3) \times 10^{-15} \text{ s}^{-2} \\
 \ddot{f} &= 1.9283(14) \times 10^{-23} \text{ s}^{-3} \\
 \dddot{f} &= 6.39(25) \times 10^{-33} \text{ s}^{-4} \\
 f^{(4)} &= -2.1(2) \times 10^{-40} \text{ s}^{-5} \\
 f^{(5)} &= 3(3) \times 10^{-49} \text{ s}^{-5}
 \end{aligned} \tag{1}$$

Here the number in parenthesis is a conservative estimate of the formal  $1\sigma$  error on the measured best-fit value, taking into account the correlations between parameters (see TACL for details). It should be noted that the best-fit value for the fourth derivative quoted earlier by Arzoumanian *et al.* (1996) and used in JR97,  $f^{(4)} = -2.1(6) \times 10^{-40} \text{ s}^{-5}$ , has not changed, while the estimated  $1\sigma$  error has decreased by a factor of three. This gives us confidence that the new measurement of  $f^{(5)}$ , although preliminary, will not change significantly over the next few years as more timing data become available.

Since the orbital period of the second companion is much longer than that of the inner binary, we treat the inner binary as a single object. Keeping the same notation as in JR97, we let  $m_1 = m_{\text{NS}} + m_c$  be the mass of the inner binary pulsar, with  $m_{\text{NS}}$  the mass of the neutron star and  $m_c$  the mass of the (inner) companion, and we denote by  $m_2$  the mass of the second companion. The orbital parameters are the longitude  $\lambda_2$  at epoch (measured from pericenter), the longitude of pericenter  $\omega_2$  (measured from the ascending node), the eccentricity  $e_2$ , semimajor axis  $a_2$ , and inclination  $i_2$  (such that  $\sin i_2 = 1$  for an orbit seen edge-on). They all refer to the orbit of the second companion with respect to the center of mass of the system (the entire triple). A subscript 1 for the orbital elements refers to the orbit of the inner binary. We assume that  $m_{\text{NS}} = 1.35 M_{\odot}$ , giving  $m_c \sin i_1 = 0.3 M_{\odot}$ , where  $i_1$  is the inclination of the pulsar binary (Thorsett *et al.* 1993), and we take  $\sin i_1 = 1$  for the analysis presented in this section since our results depend only very weakly on the inner companion mass.

The observed value of  $\dot{f}$  is in general determined by a combination of the intrinsic spin-down of the pulsar and the acceleration due to the second companion. However, in this case, the observed value of  $\dot{f}$  has changed from  $-8.1 \times 10^{-15} \text{ s}^{-2}$  to  $-5.4 \times 10^{-15} \text{ s}^{-2}$  over eleven years (TACL). Since the intrinsic spin-down rate is essentially constant, this large observed rate of change indicates that the observed  $\dot{f}$  is almost entirely acceleration-induced. Similarly, the observed value of  $\ddot{f}$  is at least an order of magnitude larger than the estimate of  $\ddot{f}$  from intrinsic timing noise, which is usually not measurable for old millisecond pulsars (see Arzoumanian *et al.* 1994, TACL, and JR97). Intrinsic contributions to the higher derivatives should also be completely negligible for millisecond pulsars. Hence, in our analysis, we assume that all observed frequency derivatives are dynamically induced, reflecting the presence of the second companion.

Fig. 1 illustrates our new one-parameter family of solutions, or “standard solution,” obtained using the updated values of the first four pulse frequency derivatives. There are no significant differences compared to the solution obtained previously in JR97. The vertical solid line indicates the unique solution obtained by including the fifth derivative. It corresponds to a second companion mass  $m_2 \sin i_2 = 7.0 \times 10^{-3} M_\odot$ , eccentricity  $e_2 = 0.45$ , and semimajor axis  $a_2 = 57$  AU. For a total system mass  $m_1 + m_2 = 1.65 M_\odot$  this gives an outer orbital period  $P_2 = 308$  yr.

It is extremely reassuring to see that the new measurement of  $f^{(5)}$  is consistent with the family of solutions obtained previously on the basis of the first four derivatives. The implication is that the signs and magnitudes of these five independently measured quantities are all consistent with the basic interpretation of the data in terms of a second companion orbiting the inner binary pulsar in a Keplerian orbit.

For comparison, the two vertical dashed lines in Fig. 1 indicate the change in the solution obtained by decreasing the value of  $f^{(5)}$  by a factor of 1.5 (right), or increasing it by a factor of 1.5 (left). Note that lower values of  $f^{(5)}$  give higher values for  $m_2$ . If we vary the value of  $f^{(5)}$  within its entire  $1\sigma$  error bar, all solutions are allowed, except for the extremely low-mass solutions with  $m_2 \lesssim 0.002$ . In particular, the present  $1\sigma$  error on  $f^{(5)}$  does not strictly rule out a hyperbolic orbit ( $e_2 > 1$ ) for  $m_2$ . However, it is still possible to derive a strict upper limit on  $m_2$  by considering hyperbolic solutions and requiring that the relative velocity at infinity of the perturber be less than the escape speed from the cluster core. This will be discussed in §2.3. A strict *lower limit* on the mass,  $m_2 \gtrsim 2 \times 10^{-4} M_\odot$ , can be set by requiring that the orbital period of the second companion be longer than the duration of the timing observations (about 10 yr). Note that all solutions then give dynamically stable triples, even at the low-mass, short period limit (see JR97 for a more detailed discussion).

## 2.2. Orbital Perturbations

Additional constraints and consistency checks on the model can be obtained by considering the perturbations of the orbital elements of the inner binary due to the presence of the second companion. These include a precession of the pericenter, as well as short-term linear drifts in the inclination and eccentricity. The drift in inclination can be detected through a change in the projected semimajor axis of the pulsar. The semimajor axis itself is not expected to be perturbed significantly by a low-mass second companion (Sigurdsson 1995).

The latest measurements, obtained by adding a linear drift term to each orbital element in the Keplerian fit for the inner binary (TACL) give:

$$\dot{\omega}_1 = -5(8) \times 10^{-5} \text{ } \circ \text{ yr}^{-1}, \quad (2)$$

$$\dot{e}_1 = 0.2(1.1) \times 10^{-15} \text{ s}^{-1}, \quad (3)$$

$$\dot{x}_p = -6.7(3) \times 10^{-13}, \quad (4)$$

where  $x_p = a_p \sin i_1$  is the projected semimajor axis of the pulsar. Note that only  $\dot{x}_p$  is clearly detected, while the other two measurements only provide upper limits.

We use these measurements to constrain the system by requiring that all our solutions be consistent with these secular perturbations. To do this, we perform Monte-Carlo simulations, constructing a large number of random realizations of the triple system in 3D, and accepting or rejecting them on the basis of compatibility with the measured orbital perturbations (see JR97 for details). The eccentricity of the outer orbit is selected randomly assuming a thermal distribution, and the other orbital parameters are then calculated from the standard solutions obtained in §2.1 (see below for a modified procedure which includes the preliminary measurement of  $f^{(5)}$ ). The unknown inclination angles  $i_1$  and  $i_2$  are generated assuming random orientations of the orbital planes, and the two position angles of the second companion are determined using  $i_1$ ,  $i_2$ ,  $\omega_2$ ,  $\lambda_2$ , and an additional undetermined angle  $\alpha$ , which (along with  $i_1$  and  $i_2$ ) describes the relative orientation of the two orbital planes. The perturbations are calculated theoretically for each realization of the system, assuming a fixed position of the second companion. The perturbation equations are given in Rasio (1994) and JR97.

Fig. 2 shows the resulting probability distributions for the mass  $m_2$  and the current separation (at epoch)  $r_{12}$  of the second companion. The Monte-Carlo trials were performed using only our standard solution based on four pulse frequency derivatives, since the fifth derivative is still only marginally detected. The solid line indicates the value given by the preliminary measurement of  $f^{(5)}$ . The most probable value of  $m_2 \simeq 0.01M_\odot$  is consistent with the range of values obtained from the complete solution using the fifth derivative. The two dashed lines indicate the values obtained from the complete solution by decreasing the value of  $f^{(5)}$  by a factor of 1.5 (right), or increasing it by a factor of 1.5 (left).

Fig. 3 shows the probability distribution of  $f^{(5)}$  predicted by our Monte-Carlo simulations, with the vertical solid line indicating the preliminary measurement, and the dashed lines showing the values of  $f^{(5)}$  increased and decreased by a factor of 1.5, as before. The most probable value is clearly consistent with the measured value, well within the formal  $1\sigma$  error. This result provides another independent self-consistency check on our model, indicating that all the present timing data, including the orbital perturbations, are consistent with the basic interpretation of the system in terms of a triple.

Since the uncertainty in  $f^{(5)}$  is still large, it can also be included in the Monte-Carlo procedure as a new constraint, in addition to the three orbital perturbation parameters. For each realization of the system, we now also calculate the predicted value of  $f^{(5)}$ , and we add compatibility with the measured value (assuming a Gaussian distribution around the best-fit value, with the quoted  $1\sigma$  standard deviation) as a condition to accept the system. These Monte-Carlo simulations with the additional constraint on  $f^{(5)}$  produce results very similar to those of Fig. 2, giving in particular the same value for the most probable second companion mass. This is of course not surprising, given the results of Fig. 3. The only significant difference is that the small number of accepted

solutions with  $m_2 \lesssim 10^{-3}M_{\odot}$  seen in Fig. 2 (small hump seen on the left of the main peak) are no longer allowed.

We also conducted Monte-Carlo simulations using  $f^{(5)}$  *alone* as a constraint, to determine the *a priori* probability distributions of the three secular perturbations for solutions that are consistent with all measured pulse frequency derivatives. Fig. 4 shows the distribution of the absolute values of the three secular perturbations (the symmetry of the problem allows both positive and negative values with equal probability) that were consistent with the frequency derivative data. We see that the allowed values of the perturbations span several orders of magnitude, with the most probable values of  $\dot{x}_p$ ,  $\dot{e}_1$ , and  $\dot{\omega}_1$  being roughly consistent with their observed values.

We note from Fig. 4 that the wide probability distribution for  $\dot{x}_p$  easily allows (although it does not favor) values much smaller than its currently observed value. This suggests the possibility that the observed value of  $\dot{x}_p$  may be significantly affected by external effects, such as the proper motion of the pulsar (which, if significant, can also lead to a slow drift in the inclination of the orbital plane to the line of sight, through the change in the direction of the line of sight itself). Indeed this possibility was discussed by Arzoumanian *et al.* (1996). They pointed out that, if the pulsar proper motion is equal to the published cluster proper motion,  $\mu = 19.5 \text{ mas yr}^{-1}$  (Cudworth & Hansen 1993) and if the proper motion alone determines the measured  $\dot{x}_p$ , this would require the inclination angle  $i_1$  to be less than about  $16^\circ$ , implying a mass  $\gtrsim 1.4 M_{\odot}$  for the (inner) pulsar companion. While another neutron star, or a black hole companion cannot be strictly ruled out, this would require a highly unusual formation scenario for the system, and would make the nearly circular orbit of the binary pulsar extremely difficult to explain.

Note, however, that the published cluster proper motion may be in error. Indeed, the pulsar timing proper motion obtained by TACL,  $\mu = 28.4 \text{ mas yr}^{-1}$ , is incompatible with the published value for the cluster, since it would imply a relative velocity of the pulsar system with respect to the cluster of  $78 \pm 40 \text{ km s}^{-1}$  (TACL), far greater than the escape speed from the cluster. Since the location of the pulsar very near the cluster core makes its association with the cluster practically certain, it is very likely that either the timing proper motion or the cluster proper motion is incorrect (see TACL for further discussion).

If we assumed that the observed  $\dot{x}_p$  is due entirely to proper motion, we can obtain an estimate of the proper motion. For example, take the inner pulsar companion to be a white dwarf of mass  $0.35 M_{\odot}$ , corresponding to an inclination  $i_1 = 55^\circ$ . We find that this would require a proper motion  $\mu \simeq 100 \text{ mas yr}^{-1}$ , or about five times greater than the current value of the optical (cluster) proper motion, and implying a velocity far greater than the escape speed for the cluster. But this is also about four times greater than the pulsar timing proper motion obtained by TACL. Therefore, if the observed  $\dot{x}_p$  were due to proper motion, then *both* the optical and timing proper motion would have to be incorrect, which seems unlikely.

### 2.3. Hyperbolic Solutions

Given the uncertainty in the proper motion of the system and the fact that the measurements of  $f^{(5)}$  and the orbital perturbations would allow it, we have also considered the possibility that the “second companion” may in fact be an object on a hyperbolic orbit, caught in the middle of a close interaction with the binary pulsar. The probability of observing the system during such a transient event is of course very low ( $\sim 2 \times 10^{-5}$  if the binary pulsar is in the core of M4; see Phinney 1993), but it cannot be ruled out a priori.

In Fig. 5, we show the predicted value of  $f^{(5)}$  as a function of the mass of the second companion ( $m_2 \sin i_2$ ), obtained by extending the solutions of Fig. 1 into the hyperbolic domain. Values of  $m_2 \sin i_2 > 0.012 M_\odot$  correspond to a hyperbolic orbit for the second companion ( $e_2 > 1$ ). The solid horizontal line indicates the measured value of  $f^{(5)}$ , and the dashed lines indicate the current  $1\sigma$  error bar. We see that the current uncertainty in  $f^{(5)}$  allows the entire range of hyperbolic orbits for the second companion.

However, a strict upper limit on  $m_2$  can be derived from the requirement that the pulsar remain bound to the cluster. For  $m_2 \sin i_2 > 0.055 M_\odot$ , we find that the relative velocity (“at infinity”) would exceed the escape speed from the cluster core ( $\simeq 12 \text{ km s}^{-1}$ ; see Peterson *et al.* 1995). To reach a stellar mass, say  $m_2 = 0.5 M_\odot$ , would require a relative velocity at infinity  $\simeq 45 \text{ km s}^{-1}$ , which would be well above the escape speed from the cluster. Thus, even in the hyperbolic regime, the mass of the second companion is constrained to remain substellar. In addition, we find that the hyperbolic solutions require the present position of the second companion to be very close to pericenter ( $|\lambda_2| < 10^\circ$ ). This is not surprising, since the hyperbolic solutions are a smooth extension of the standard bound solutions shown in Fig. 1 (in which  $\lambda_2$  is already small for solutions with  $e_2 \simeq 1$ ), but it makes the hyperbolic solutions even more unlikely.

## 3. Triple Formation Process

### 3.1. Recycling in the Triple

One plausible formation scenario for PSR B1620–26 begins with an old neutron star in a binary system, which has a dynamical interaction with a star–planet system (Sigurdsson 1993, 1995). The original companion of the neutron star is ejected in the interaction, while the main-sequence star and its orbiting giant planet are retained in orbit around the neutron star. The planet is typically retained in a wider orbit around the new inner binary system. The main-sequence star later evolves to become a red giant, transferring mass onto the neutron star and recycling it into a millisecond pulsar, while at the same time the inner orbit is circularized through tidal dissipation. Thus, in this scenario, the triple system is formed before the recycling of the neutron star takes place.

Sigurdsson (1993) finds through numerical scattering experiments, that in approximately 15%

of such exchange interactions (in which the main-sequence star remains bound to the neutron star), the planet is left in a bound, wide orbit around the system. In a majority of such cases, the planet has a final semimajor axis 10 – 100 times larger than the initial semimajor axis of the neutron star binary, and an eccentricity in the range 0.3 – 0.7. Sigurdsson (1993) also finds that the probability of retaining a planet is proportionately higher if the main-sequence star has more than one planet orbiting it. Thus it seems reasonable to consider such an exchange interaction as a possible formation scenario for PSR B1620–26.

However, there are two main difficulties with this scenario. First, it requires that the age of the millisecond pulsar be at most comparable to the age of the triple system. Our modeling of the timing data (§2) indicates that the semimajor axis of the planet’s orbit is  $\gtrsim 50$  AU. This makes the outer orbit of the triple “soft” in the cluster, implying that any close interaction with a passing star will disrupt the triple (ejecting the planet). Since gravitational focusing is negligible for such a large object, the lifetime of the triple can then be written

$$\tau_d \simeq 8.5 \times 10^7 \text{ yr} \eta_d^2 \left( \frac{\langle m \rangle}{0.8 M_\odot} \right) \left( \frac{10^4 M_\odot \text{ pc}^{-3}}{\rho} \right) \left( \frac{5 \text{ km s}^{-1}}{\sigma} \right) \left( \frac{50 \text{ AU}}{a_2} \right)^2. \quad (5)$$

Here  $\langle m \rangle$  is the average stellar mass in the cluster,  $\rho$  is the stellar density,  $\sigma$  is the 3D velocity dispersion,  $a_2$  is the semimajor axis of the outer orbit, and  $\eta_d \equiv a_2/r_d$ , where  $r_d$  is the average distance of closest approach for an encounter that will disrupt the outer orbit. Based on an extensive set of scattering experiments (see §3.2 below), we find that  $r_d/a_2 \simeq 1.4$  and therefore the factor  $\eta_d^2 \simeq 0.5$ . Hence, in the core of M4, the expected lifetime of the triple is  $\tau_d \sim 3 \times 10^7$  yr. This is much shorter than the estimated age of the binary pulsar,  $\tau_p \gtrsim 10^9$  yr (Thorsett *et al.* 1993). However, outside the core, the expected lifetime of the triple can be up to two orders of magnitude longer due to the much lower number density of stars in the halo. For example, at the half-mass radius of M4, the stellar density is down to  $\sim 10^2 M_\odot \text{ pc}^{-3}$  and the lifetime becomes  $\tau_{\text{hm}} \sim 10^9$  yr. Hence, this scenario would require that the triple system, currently observed (in projection) near the edge of the cluster core, is in fact on an orbit that extends far outside the core, allowing it to spend most of its lifetime in the less dense cluster halo.

Indeed, Sigurdsson (1995) showed through numerical simulations, that a triple system with a low-mass second companion, such as PSR B1620–26, is more likely to be observed outside the cluster core than inside the core. Sigurdsson also finds that such triples can easily survive for up to  $2 \times 10^9$  yr by spending most of their time outside the core, but that once they enter the core, they are quickly disrupted. In contrast, triples with stellar-mass second companions sink to the core much more quickly due to dynamical friction (on a timescale  $\lesssim 10^9$  yr), and have a lifetime of order  $10^8$  yr in the core (Sigurdsson 1995, Rasio *et al.* 1995). Thus the fact that PSR B1620–26 is observed just outside the core suggests that it probably contains a low-mass second companion (which is consistent with our timing solution), or that it is a very young system formed less than  $5 \times 10^8$  yr ago (which is difficult to reconcile with the estimated age of the binary pulsar in this scenario).

The other difficulty concerns the eccentricity of the pulsar binary. Since the circularization of the inner binary takes place after the triple is formed, this scenario leaves the higher observed eccentricity of the inner binary unexplained. To produce the higher eccentricity, a second dynamical interaction of the triple with a passing star can be invoked (Sigurdsson 1995). However, a very close interaction is needed to induce a significant eccentricity in an initially circular binary (Rasio, McMillan, & Hut 1995; see Heggie & Rasio 1996 for a general treatment of this problem). Therefore, such an encounter is likely to disrupt the outer orbit in the triple system. An encounter with a distance of closest approach of  $\simeq 2.5$  AU to the inner binary could induce the observed eccentricity. But this is much smaller than the semimajor axis of the outer orbit, and roughly half of such encounters will disrupt the outer orbit (Sigurdsson 1995). Such a close interaction occurs on average once in  $\sim 4 \times 10^8$  yr. Therefore, for each interaction that could have produced the eccentricity of the inner binary, we expect  $\sim 10$  encounters that could have disrupted the outer orbit, leaving the probability of surviving at  $\lesssim 0.01$ .

Alternatively, it is possible that the eccentricity of the inner orbit could have been induced later through secular perturbations in the triple. Rasio (1994) argued that this is unlikely for a low-mass second companion with low relative inclination between the two orbits. However, we find that under certain conditions, the inner eccentricity can be explained as arising from the combined effects of the tidal perturbation by the second companion and the general relativistic precession of the inner orbit. We discuss this in more detail in § 4.

### 3.2. Pre-Existing Binary Pulsar

We now propose an alternative formation scenario, which involves a dynamical exchange interaction between a *pre-existing* binary millisecond pulsar and another wider system containing a giant planet in orbit around a main-sequence star. This interaction could lead to the ejection of the main-sequence star, leaving the planet in a wide orbit around the binary pulsar. An exchange interaction of this type might also simultaneously induce the observed eccentricity of the binary pulsar if either the main-sequence star or the planet passes sufficiently close to the binary pulsar during the interaction. This scenario is a natural extension of the mechanism studied by Rasio *et al.* (1995) for the formation of a stellar triple containing a millisecond pulsar. Here, however, an added difficulty is that one expects the planet, and not the main-sequence star, to be preferentially ejected during the interaction.

To study this binary-binary interaction scenario quantitatively, we have performed numerical scattering experiments similar to those done by Rasio, McMillan, & Hut (1995) for stellar triples. The binary pulsar was treated as a single body of mass  $1.65 M_{\odot}$ , scattering off several different binary systems containing a main-sequence star with a very low-mass companion (which we refer to henceforth as the “star–planet system”). The assumption that one can treat the inner pulsar binary as a single mass is justified because its semimajor axis (0.77 AU) is considerably smaller than the orbital radius of the planet in all relevant cases. In addition, close approaches to the

binary pulsar by either the planet or the main-sequence star are forbidden, since they would induce an eccentricity larger than the one observed. For example, an approach by a  $0.01 M_{\odot}$  object to within about 1.2 AU (1.5 semimajor axes) of the pulsar binary would be enough to induce an eccentricity greater than 0.025 (cf. Heggie & Rasio 1996). Hence in all relevant interactions, the pulsar binary could be treated as a single point mass.

Four different outcomes are possible for each simulated interaction: (1) ionization; (2) no exchange (as in a flyby); (3) exchange in which the planet is retained around the binary pulsar; (4) exchange in which the star remains bound to the binary pulsar. Exchanges can be further divided into “resonant” and “nonresonant” or “direct.” In a resonant exchange interaction, all stars involved remain together for a time long compared to the initial orbital periods (typically  $\sim 10^2 - 10^3$  dynamical times), leading eventually to the ejection of one object while (in this case) the others remain in a bound hierarchical triple configuration. In direct exchange interactions, either the planet or the main-sequence star is ejected promptly, following a close approach by the binary pulsar. In general, the type of outcome depends on the impact parameter, the mass of the planet, and the initial planet-star separation.

Heggie, Hut, & McMillan (1996) have computed cross sections for exchange interactions in binary-single-star encounters, both numerically using scattering experiments, and analytically in various limiting regimes. They include results for binary mass ratios as extreme as  $\sim 0.01$ . However, their results are all obtained for *hard* binaries, whereas the star–planet system in our scenario represents a very soft binary. Therefore, we do not expect the results of Heggie *et al.* (1996) to be directly applicable here, although they do provide some qualitative predictions. For example, for a binary mass ratio  $m_2/m_1 \simeq 0.01$ , and  $m_3/m_1 = 1$ , the ratio of cross sections for ejection of the star ( $m_1$ ) to ejection of the planet ( $m_2$ ) is about 0.12 for direct exchanges and 0.04 for resonant exchanges, with the total cross section for all resonant exchanges being about 2.5 times larger than that of all direct exchanges. For soft binaries we find that direct exchanges are dominant and that the relative probability of ejecting the more massive binary member is higher (see below).

Our scattering experiments were performed using the **scatter3** module of the STARLAB stellar dynamics package (McMillan & Hut 1996; Portegies Zwart *et al.* 1997). The mass of the main-sequence star was held constant at  $0.8 M_{\odot}$ , close to the main-sequence turn-off point of the cluster. The planet was placed on an initially circular orbit. The relative velocity at infinity for all encounters was taken to be  $4 \text{ km s}^{-1}$ , slightly lower than the 3D velocity dispersion in the cluster core ( $\simeq 6 \text{ km s}^{-1}$ ; see Peterson *et al.* 1995). The impact parameter  $b$  was randomly selected between zero and  $b_{\max}$ , with probability  $p(b) \propto 2\pi b$ . The upper limit was selected such that all interactions with  $b \geq b_{\max}$  led to a fly-by with no exchange. In units of the initial semimajor axis of the star–planet system,  $b_{\max}$  varied from about 5 to 35 depending on the mass of the planet. Three different masses were selected for the “planet.”  $0.001 M_{\odot}$ ,  $0.01 M_{\odot}$ , and  $0.1 M_{\odot}$ . In each case, the semimajor axis of the star–planet system was initially chosen to be 5 AU, since this is the typical distance at which giant planets are expected to form. In addition, in an effort to better

match the orbital parameters of triple systems like PSR B1620–26, we also considered initial star–planet semimajor axes of 30 AU and 50 AU.

We first address the possibility of capturing the planet into a wide orbit around the pulsar binary, while ejecting the star during an exchange interaction. Fig. 6 shows the distributions of the semimajor axis and eccentricity of the planet in the triple for those interactions in which the planet was captured and the binary pulsar was not disrupted. We see that the final semimajor axis of the planet in the triple is likely to be within a factor of  $\sim 2$  of the initial star–planet separation  $a_p$  (Note that, in this section, an index  $p$  refers to the orbit of the star–planet system, and not to the pulsar, as in §2). The eccentricity distribution is very broad, and approaches a “thermal” distribution ( $p(e) \propto e$ ) for very wide initial separations.

Fig. 7(a)–(e) shows the corresponding probabilities of the three possible outcomes (branching ratios) for different planet masses and initial separations of the star–planet system. The distance of closest approach  $r_p$  is given in units of the initial star–planet semimajor axis  $a_p$ . Since the planet was the lowest-mass object participating in the interaction, it was expected to have a much higher probability of being ejected. However, we find that the branching ratio for interactions resulting in the capture of the planet remains significant for all interactions close enough to result in an exchange. For example, from Fig. 7(e), we see that for an interaction between the binary pulsar and a star–planet system with separation 50 AU and planet mass  $m_p = 0.01 M_\odot$ , the branching ratio for planet capture (ejection of the star) is in the range  $\simeq 10 – 30\%$  for distances of closest approach in the range  $\sim 10 – 50$  AU. For this case, there are no resonant interactions, implying that retention of the star has negligible probability, while the branching ratio for ionization is in the range  $\simeq 20 – 60\%$ . The remainder of the interaction cross section (10% to 70%) corresponds to “clean” flyby’s (without capture of either star or planet, or ionization).

To focus our study on interactions in which the final triple configuration is similar to that of PSR B1620–26, we now eliminate cases in which the eccentricity induced in the binary pulsar’s orbit would have been larger than the present value of 0.025. The induced eccentricity is estimated based on the results of Heggie & Rasio (1996). In making these estimates, all unknown angles, including the relative inclination of the two orbits, are chosen randomly (assuming random orientations). Frames (f)–(j) in Fig. 7 show the branching ratios for those interactions in which the eccentricity induced in the binary pulsar during the interaction is below 0.025. The main difference with the general results (frames (a)–(e) in Fig. 7) is that the branching ratio for ejection of the star now goes to zero for very close interactions, since those interactions in which the star passes very close to the binary pulsar would have induced an eccentricity larger than allowed. Fig. 8 shows the corresponding distributions of semimajor axis and eccentricity of the planet in the triple (like Fig. 6 but with the additional constraint on induced eccentricity). Here the only significant difference is in the lower probability of retaining the planet on a highly eccentric orbit, especially for more massive planets (compare, e.g., Fig. 8c to Fig. 6c).

In Table 1, we list the cross sections for the various outcomes, obtained from our scattering

experiments for each of the five cases. The cross sections are given in units of the initial geometrical cross section of the star–planet binary ( $\pi a_p^2$ ).

We now turn to the question of whether the eccentricity of the binary pulsar could have been increased significantly during the interaction. Fig. 9 shows the overall distribution of the final eccentricity induced in the binary pulsar following an exchange interaction in which the planet was retained. In every case, we see that the induced eccentricity varies over a large range, including the currently observed eccentricity of the binary pulsar. Thus, a scenario in which an exchange interaction successfully forms the triple *and* simultaneously induces the inner binary eccentricity we see today is certainly possible, although the present value of the eccentricity is not likely in this scenario. Alternatively, the triple could have formed with an initial inner binary eccentricity *lower* than the present value. The eccentricity could then be raised to the present value by long-term secular perturbation effects (§4). Forming the triple with an initial inner binary eccentricity *higher* than currently observed and later reducing it through secular perturbations is also possible.

Our analysis of the PSR B1620–26 timing data (§2) indicate that the second companion is in a wide orbit around the pulsar binary, with a semimajor axis  $\gtrsim 50$  AU. The results of our scattering experiments indicate that the final semimajor axis of the planet in the triple should be comparable to the initial star–planet separation (see Figs. 6 and 8). Hence, the interactions that could have produced a system like PSR B1620–26 are those involving a wide system with a planet mass  $m_p \sim 0.01 M_\odot$  and an initial separation  $a_p \sim 50$  AU, as shown in Figs. 7(j) and 8(e). Just like the triple itself, such a wide star–planet system is “soft” (binding energy smaller than the typical center-of-mass energy of an encounter) and has a large interaction cross section, implying a short lifetime in the cluster core,  $\tau_d \sim 3 \times 10^7$  yr (cf. eq. 5). Well outside of the cluster core, its lifetime could be much longer, but since an exchange interaction with another binary is likely to take place only in the core, it requires the star–planet system to first drift into the core through dynamical friction. The interaction that destroyed the star–planet system once it entered the core could be the one that produced the PSR B1620–26 triple.

#### 4. Secular Eccentricity Perturbations

We now examine in detail the possibility that the inner binary eccentricity was induced by the secular gravitational perturbation of the second companion. In the hierarchical three-body problem, analytic expressions for the maximum induced eccentricity and the period of long-term eccentricity oscillations are available in certain regimes, depending on the eccentricities and relative inclination of the orbits.

#### 4.1. Planetary Regime

For orbits with small eccentricities and a small relative inclination ( $i \lesssim 40^\circ$ ), the classical solution for the long-term secular evolution of eccentricities and longitudes of pericenters can be written in terms of an eigenvalue and eigenvector formulation (Brouwer & Clemence 1961; for an excellent pedagogic summary, see Dermott & Nicholson 1986). This classical solution is valid to all orders in the ratio of semimajor axes. In this regime the eccentricities oscillate as angular momentum is transferred between the two orbits. The precession of the orbits (libration or circulation) is coupled to the eccentricity oscillations, but the relative inclination remains approximately constant. In this regime it can be shown that a stellar mass second companion would be necessary to induce the observed eccentricity in the inner binary (Rasio 1994; 1995). Such a large mass for the third body has been ruled out by recent timing data (See §2), implying that secular perturbations from a third body in a nearly coplanar and circular orbit does not explain the observed inner eccentricity. The lack of a stellar-mass companion is also supported by the absence of an optical counterpart for the pulsar in the HST observations by Bailyn *et al.* (1999).

Sigurdsson (1995) has suggested that it may be possible for the secular perturbations to grow further because of random distant interactions of the triple with other cluster stars at distances  $\sim 100$  AU, which would perturb the long-term phase relation between the inner and outer orbits, allowing the inner eccentricity to “random walk” up to a maximum value up to two orders of magnitude higher than that predicted for an isolated triple. However, the current most probable solution from the timing data requires the the second companion to be in a very wide orbit (separation  $\gtrsim 40$  AU), giving it a very short lifetime in the core, and leaving it extremely vulnerable to disruption by repeated weak encounters (see JR97 for a more detailed discussion).

#### 4.2. High-Inclination Regime

For a triple system formed through a dynamical interaction, there is no reason to assume that the relative inclination of the two orbits should be small. When the relative inclination of the two orbital planes is  $\gtrsim 40^\circ$ , a different regime of secular perturbations is encountered. This regime has been studied in the past using the quadrupole approximation (Kozai 1962; see Holman, Touma, & Tremaine 1987 for a recent discussion). Here the relative inclination  $i$  of the two orbits and the inner eccentricity  $e_1$  are coupled by the integral of motion (Kozai’s integral)

$$\Theta = (1 - e_1^2) \cos^2 i. \quad (6)$$

Thus, the amplitude of the eccentricity oscillations is determined by the relative inclination. It can be shown that large-amplitude eccentricity oscillations are possible only when  $\Theta < 3/5$  (Holman *et al.* 1997). For an initial eccentricity  $e_1 \simeq 0$  and initial inclination  $i_0$  this implies

$i_0 > \cos^{-1} \sqrt{3/5} \simeq 40^\circ$  and the maximum eccentricity is then given by

$$e_{1\max} = \left(1 - \frac{5}{3} \cos^2 i_0\right)^{1/2}, \quad (7)$$

which approaches unity for relative inclinations approaching  $90^\circ$ . For a sufficiently large relative inclination, this suggests that it should always be possible to induce an arbitrarily large eccentricity in the inner binary, and that this could provide an explanation for the anomalously high eccentricity of the binary pulsar in the PSR B1620–26 system (Rasio, Ford, & Kozinsky 1997). However, there are two additional conditions that must be satisfied for this explanation to hold.

First, the timescale for reaching a high eccentricity must be shorter than the lifetime of the system. Although the masses, initial eccentricities, and ratio of semimajor axes do not affect the maximum inner eccentricity, they do affect the period of the eccentricity oscillations (see Holman *et al.* 1997; Mazeh *et al.* 1996). The inner longitude of periastron precesses with this period, which can be quite long, sometimes exceeding the lifetime of the system in the cluster. The masses also affect the period, but they decrease the amplitude of the eccentricity oscillations only when the mass ratio of the inner binary approaches unity (Ford, Kozinsky, & Rasio 1999). In Fig. 10 we compare the period of the eccentricity oscillations to the lifetime of the triple in M4 (see §4.3 for details on how the various estimates were obtained). It is clear that for most solutions the timescale to reach a large eccentricity exceeds the lifetime of the triple. The only possible exceptions are for very low-mass planets ( $m_2 \lesssim 0.002 M_\odot$ ) and with the triple residing far outside the cluster core. These cannot be excluded, but are certainly not favored by the observations (see §2).

The second problem is that other sources of perturbations may become significant over these long timescales. In particular, for an inner binary containing compact objects, general relativistic effects can become important. This turns out to play a crucial role for the PSR B1620–26 system, and will be discussed in detail in the next section.

### 4.3. General Relativistic Effects

Additional perturbations which alter the longitude of periastron can indirectly affect the evolution of the eccentricity of the inner binary in a hierarchical triple. For example, tidally- or rotationally-induced quadrupolar distortions, as well as general relativity, can cause a significant precession of the inner orbit for a sufficiently compact binary. If this additional precession is much slower than the precession due to the secular perturbations, then the eccentricity oscillations are not significantly affected. However, if the additional precession is faster than the secular perturbations, then eccentricity oscillations are severely damped (Holman *et al.* 1997; Lin *et al.* 1998). In addition, if the two precession periods are comparable, then a type of resonance can occur that leads to a significant increase in the eccentricity perturbation (Ford *et al.* 1999).

Fig. 10 compares the various precession periods for PSR B1620-26 as a function of the second companion mass  $m_2$  for the entire one-parameter family of standard solutions constructed in §2. Also shown for comparison is the lifetime of the triple, both in the cluster core and at the half-mass radius. We assumed that the stellar densities in the core and at the half-mass radius are  $10^4 M_\odot \text{ pc}^{-3}$  and  $10^2 M_\odot \text{ pc}^{-3}$ , with average stellar masses  $\langle m \rangle = 0.8 M_\odot$  and  $0.3 M_\odot$ , respectively, and set the 3D velocity dispersions to  $6 \text{ km s}^{-1}$  in the core and  $3 \text{ km s}^{-1}$  at the half-mass radius. Disruption of the triple is assumed to occur for any encounter with pericenter distance smaller than  $a_2$  (corresponding to setting  $\eta_d = 1$  in eq. 5). The timescale between such encounters was then estimated from simple kinetic theory (see, e.g., eq. 8-123 of Binney & Tremaine 1987), taking into account gravitational focusing (which is significant at the low-mass, short-period end of the sequence of solutions; instead, our eq. 5 is valid in the limit where gravitational focusing is negligible). The precession period  $P_{\text{High } i}$  for high-inclinations was calculated using the approximate analytic expression given by Holman *et al.* (1997, eq. 3), while  $P_{\text{Low } i}$  is from Brouwer & Clemence (1961; see Rasio 1995 for simplified expressions in various limits). The general relativistic precession period,  $P_{\text{GR}}$  is derived, e.g., in Misner, Thorne, & Wheeler (1973; §40.5). Note that, although we have labeled the plot assuming  $\sin i_2 = 1$ , only  $P_{\text{Low } i}$  has an explicit dependence on  $m_2$  (and it is calculated here for  $\sin i_2 = 1$ ).

For nearly all solutions we find that the general relativistic precession is *faster* than the precession due to the Newtonian secular perturbations. The only exceptions are for low-mass second companions ( $m_2 \lesssim 0.005 M_\odot$ ) in low-inclination orbits. However, we have already mentioned above (§4.1) that in this case the maximum induced eccentricity cannot reach the present observed value (for detailed calculations, see Rasio 1994, 1995, and §4.4).

Most remarkably, we see immediately in Fig. 10 that for the most probable solution (based on the current measured value of  $f^{(5)}$  and indicated by the vertical solid line in the figure), the two precession periods are *nearly equal* for a low-inclination system. This suggests that resonant effects may play an important role in this system, a possibility that we have explored in detail using numerical integrations. We describe the numerical results in the next section.

#### 4.4. Numerical Integrations of the Secular Evolution Equations

If the quadrupole approximation used for the high-inclination regime is extended to octupole order, the resulting secular perturbation equations approximate very well the long-term dynamical evolution of hierarchical triple systems for a wide range of masses, eccentricities, and inclinations (Ford, Kozinsky, & Rasio 1999). We have used the octupole-level secular perturbation equations derived by Ford *et al.* (1999) to study the long-term eccentricity evolution of the PSR B1620-26 triple. We integrate the equations using the variables  $e_1 \sin \omega_1$ ,  $e_1 \cos \omega_1$ ,  $e_2 \sin \omega_2$ , and  $e_2 \cos \omega_2$ , where  $\omega_1$  and  $\omega_2$  are the longitudes of pericenters. This avoids numerical problems for near-circular orbits, and allows us to incorporate easily the first-order post-Newtonian correction into our integrator, which is based on the Burlish-Stoer integrator of Press *et al.* (1992).

We assume that the present inner eccentricity is due entirely to the secular perturbations and that the initial eccentricity of the binary pulsar was much smaller than its present value. In addition, we restrict our attention to the standard one-parameter family of solutions constructed in §2. From the numerical integrations we can then determine the maximum induced eccentricity, which depends only on the relative inclination.

In Fig. 11 we show this maximum induced eccentricity in the inner orbit as a function of the second companion mass for several inclinations. For most inclinations and masses, we see that the maximum induced eccentricity is significantly smaller than that the observed value, as expected from the discussion of §4.3. However, for a small but significant range of masses near the most probable value (approximately  $0.0055 M_{\odot} < m_2 < 0.0065 M_{\odot}$ ), the induced eccentricity for low-inclination systems can reach values  $\gtrsim 0.02$ .

If the initial eccentricity of the outer orbit had been larger than presently observed (as calculated in Fig. 1) but later decreased through secular perturbations, the evolution of the inner orbit may have been different. We have performed numerical integrations for this case as well and obtained results very similar to those of Fig. 11. The “resonance peaks” are slightly broader to the right side and the maximum induced eccentricity is somewhat larger when the second companion mass is large. In particular, we find that an inner eccentricity  $\gtrsim 0.02$  can then be achieved for masses as high as  $m_2 \simeq 0.012 M_{\odot}$ . However, from the results of §2 we see that the corresponding orbital separation in the standard solution is extremely large,  $a_2 \gtrsim 500$  AU, and the outer eccentricity  $e_2 \gtrsim 0.95$ , implying a very short lifetime for the triple in M4,  $\tau_d < 10^6$  yr.

For relative inclinations  $50^\circ \lesssim i \lesssim 70^\circ$  we do not find a peak in the maximum induced eccentricity as a function of  $m_2$  consistent with the timing data. For inclinations  $\gtrsim 75^\circ$  we again find a peak in the maximum induced eccentricity which becomes smaller and moves towards larger masses as the relative inclination of the two orbits is increased. A significant induced eccentricity in the inner orbit is also possible for  $m_2 \lesssim 0.004 M_{\odot}$  if the two orbits are very nearly orthogonal (cf. §4.3). However, the results of our Monte-Carlo simulations incorporating the measured value of  $f^{(5)}$  do not support this scenario.

As already pointed out in §4.3, the maximum induced eccentricity may also be limited by the lifetime of the triple system. From Fig. 10 we see that near resonance we expect  $P_{\text{Low } i} \approx P_{\text{GR}} \sim 10^7$  yr, which is comparable to the lifetime of the triple in the cluster core, and much shorter than the lifetime outside of the core. For solutions near a resonance the inner eccentricity  $e_1$  initially grows linearly at approximately the same rate as it would without the general relativistic perturbation. However, the period of the eccentricity oscillation can be many times the period of the classical eccentricity oscillations. Although this allows the eccentricity to grow to a larger value, the timescale for this growth can then be longer than the expected lifetime of the triple in the cluster core. For example, with  $m_2 = 0.006 M_{\odot}$  we find that the inner binary reaches an eccentricity of 0.025 after about 1.5 times the expected lifetime of the triple in the core of M4. Thus, even if the system is near resonance, it must still be residing somewhat outside

the core for the secular eccentricity perturbation to have enough time to grow to the currently observed value.

## 5. Summary

Our theoretical analysis of the latest timing data for PSR B1620–26 clearly confirms the triple nature of the system. Indeed, the values of all five measured pulse frequency derivatives are consistent with our basic interpretation of a binary pulsar perturbed by the gravitational influence of a more distant object on a bound Keplerian orbit. The results of our Monte-Carlo simulations based on the four well-measured frequency derivatives and preliminary measurements of short-term orbital perturbation effects in the triple are consistent with the complete solution obtained when we include the preliminary measurement of the fifth frequency derivative. This complete solution corresponds to a second companion of mass  $m_2 \sin i_2 \simeq 7 \times 10^{-3} M_\odot$  in an orbit of eccentricity  $e_2 \simeq 0.45$  and semimajor axis  $a_2 \simeq 60$  AU (orbital period  $P_2 \simeq 300$  yr). Although the present formal  $1\sigma$  error on  $f^{(5)}$  is large, we do not expect this solution to change significantly as more timing data become available.

At least two formation scenarios are possible for the triple system, both involving dynamical exchange interactions between binaries in the core of M4. In the one scenario that we have studied in detail, a pre-existing binary millisecond pulsar has a dynamical interaction with a wide star–planet system which leaves the planet bound to the binary pulsar while the star is ejected. From numerical scattering experiments we find that the probability of retaining the planet, although smaller than the probability of retaining the star, is always significant, with a branching ratio  $\simeq 10\% – 30\%$  for encounters with pericenter distances  $r_p$  in the range  $0.2 – 1a_p$ , where  $a_p \sim 50$  AU is the initial star–planet separation. All the observed parameters of the triple system are consistent with such a formation scenario, which also allows the age of the millisecond pulsar (most likely  $\gtrsim 10^9$  yr) to be much larger than the lifetime of the triple (as short as  $\sim 10^7$  yr if it resides in the core of the cluster).

It is also possible that the dynamical interaction that formed the triple also perturbed the eccentricity of the binary pulsar to the anomalously large value of 0.025 observed today. However, we have shown that through a subtle interaction between the general relativistic corrections to the binary pulsar’s orbit and the Newtonian gravitational perturbation of the planet, this eccentricity could also have been induced by long-term secular perturbations in the triple after its formation. The interaction arises from the near equality between the general relativistic precession period of the inner orbit and the period of the Newtonian secular perturbations for a low-inclination system. It allows the eccentricity to slowly build up to the presently observed value, on a timescale that can be comparable to the lifetime of the triple.

All dynamical formation scenarios have to confront the problem that the lifetimes of both the current triple and its parent star–planet system are quite short, typically  $\sim 10^7 – 10^8$  yr as they

approach the cluster core, where the interaction is most likely to occur. Therefore, the detection of a planet in orbit around the PSR B1620–26 binary clearly suggests that large numbers of these star–planet systems must exist in globular clusters, since most of them will be destroyed before (or soon after) entering the core, and most planets will not be able to survive long in a wide orbit around any millisecond pulsar system (where they may become detectable through high-precision pulsar timing). Although a star–planet separation  $a_p \sim 50$  AU may seem quite large when compared to the orbital radii of all recently detected extrasolar planets (which are all smaller than a few AU; see Marcy & Butler 1998), one must remember that the current Doppler searches are most sensitive to planets in short-period orbits, and that they could never have detected a low-mass companion with an orbital period  $\gg 10$  yr. In addition, it remains of course possible that the parent system was a primordial binary star with a low-mass, brown dwarf component, and not a main-sequence star with planets.

We are very grateful to Steve Thorsett for many useful discussions and for communicating results of observations in progress. We thank Piet Hut and Steve McMillan for providing us with the latest version of the STARLAB software. We are also grateful to C. Bailyn and S. Sigurdsson for helpful comments, and to J. Bostick for help with the calculations of §3.2. This work was supported in part by NSF Grant AST-9618116 and a NASA ATP Grant at MIT. F.A.R. was supported in part by an Alfred P. Sloan Research Fellowship. E.B.F. was supported in part by the Orloff UROP Fund and the UROP program at MIT. F.A.R. also thanks the Theory Division of the Harvard-Smithsonian Center for Astrophysics for hospitality. This work was also supported by the National Computational Science Alliance under Grant AST970022N and utilized the SGI/Cray Origin2000 supercomputer at Boston University.

## REFERENCES

Arzoumanian, Z., Fruchter, A. S., & Taylor, J. H. 1994, *ApJ*, 426, L85

Arzoumanian, Z., Joshi, K. J., Rasio, F. A., & Thorsett, S. E. 1996, in IAU Colloquium 160, *Pulsars: Problems and Progress*, ASP Conference Series Volume 105. Ed. S. Johnston *et al.* (Astronomical Society of the Pacific, San Francisco), 525

Arzoumanian, Z., Nice, D. J., Taylor, J. H., & Thorsett, S. E. 1994, *ApJ*, 422, 621

Backer, D. C. 1993, in *ASP Conf. Ser.*, 36, Planets around Pulsars, ed. Phillips J. A. *et al.* (San Francisco: ASP), 11

Backer, D. C., Foster, R. S., & Sallmen, S. 1993, *Nature*, 365, 817

Backer, D. C., & Thorsett, S. E. 1995, in *Millisecond Pulsars. A Decade of Surprise*, ASP Conf. Ser., 72 Eds. A. S. Fruchter, M. Tavani, D. C. Backer (San Francisco: ASP), 387

Bailyn, C. D., Rubinstein, E. P., Girard, T. M., Dinescu, D. I., Rasio, F. A. & Yanny, B. 1994, *ApJ*, 433, L89

Bailyn, C. D. *et al.* 1999, in preparation

Binney, J., & Tremaine, S. 1989, *Galactic Dynamics* (Princeton, PUP)

Brouwer, D. & Clemence, G. M. 1961, *Methods of Celestial Mechanics* (New York: Academic)

Butler, R. P., Marcy, G. W., Fisher, D. A., Brown, T. W., Contos, A. R., Korzennik, S. G., Nisenson, P., Noyes, R. W. 1999, *ApJ*, submitted

Cudworth, K. M. & Hansen, R. B. 1993, *AJ*, 105, 168

Dermott, S.F., & Nicholson, P.D. 1986, *Nature*, 319, 115

Ford, E. B., Kozinsky, B., & Rasio, F. A. 1999, *ApJ*, submitted

Heggie, D. C., Hut, P., & McMillan, S. L. 1996, *ApJ* 467, 359

Heggie, D. C., & Rasio, F. A. 1996, *MNRAS*, 282, 1064

Holman, M., Touma, J. & Tremaine, S. 1997, *Nature*, 386, 254

Joshi, K. J., & Rasio, F. A. 1997, *ApJ*, 479, 948. Erratum *ibid* 488, 901 (1997)

Kozai, Y., 1962, *AJ*, 67, 591

Lin, D. N. C., Papaloizou, J. C. B., Bryden, G., Ida, S., Terquem, C. 1999, to appear in “Protostars and Planets IV,” eds. A. Boss, V. Mannings, and S. Russell [astro-ph/9809200]

Lyne, A. G., Biggs, J. D., Brinklow, A., Ashworth, M., & McKenna, J. 1988, *Nature*, 332, 45

Marcy, G. W. & Butler, R. P. 1998, *ARA&A*, 36, 57

Mazeh, T., Krymolowski, Y., & Rosenfeld, G. 1996, *ApJ*, 466, 415

McKenna, J., & Lyne, A. G. 1988, *Nature*, 336, 226; erratum, 336, 698

McMillan, S. L. W., & Hut, P. 1996, *ApJ* 467, 348

Michel, F. C. 1994, *ApJ*, 432, 239

Misner, C.W., Thorne, K.S., & Wheeler, J.A. 1973, *Gravitation* (New York, Freeman)

Peterson, R. C., Rees, R. F., & Cudworth, K. M. 1995, *ApJ* 443, 124

Phinney, E. S. 1992, *Phil. Trans. R. Soc. Lond.*, A, 341, 39

Phinney, E. S. 1993, in Structure and Dynamics of Globular Clusters, ASP Conference Series, Volume 50. Ed. S. G. Djorgovski & G. Meylan (Astronomical Society of the Pacific, San Francisco), 141

Podsiadlowski, P. 1995, in Millisecond Pulsars: A Decade of Surprise, ASP Conference Series, Volume 72. Ed. A.S. Fruchter, M. Tavani, & D.C. Backer (Astronomical Society of the Pacific, San Francisco), 411

Portegies Zwart, S. F., Hut, P., McMillan, S. L. W., & Verbunt, F. 1997, *A&A* 328, 143

Press, W. H., Teukolsky, S. A., Vetterling, W. T., & Flannery, B. P. 1992, Numerical Recipes in C: The Art of Scientific Computing (2nd ed. New York: Cambridge University Press)

Rasio, F. A. 1994, *ApJ*, 427, L107

Rasio, F. A. 1995, in Millisecond Pulsars: A Decade of Surprise, ASP Conf. Series Vol. 72, eds. A.S. Fruchter et al. (ASP, San Francisco), 424

Rasio, F.A., Ford, E.B., & Kozinsky, B. 1997, AAS Meeting 191, 44.16

Rasio, F. A., & Heggie, D. C. 1995, *ApJ*, 445, L133

Rasio, F. A., McMillan, S., & Hut, P. 1995, *ApJ*, 438, L33

Shearer, A., Butler, R., Redfern, R. M., Cullum, M., & Danks, A. C. 1996, *ApJ*, 473, L115

Sigurdsson, S. 1992, *ApJ*, 399, L95

Sigurdsson, S. 1993, *ApJ*, 415, L43

Sigurdsson, S. 1995, *ApJ*, 452, 323

Stappers, B. W., Bailes, M., Lyne, A. G., Manchester, R. N., D'Amico, N., Tauris, T. M., Lorimer, D. R.; Johnston, S., & Sandhu, J. S. 1996, *ApJ*, 465, L119.

Thorsett, S. E., Arzoumanian, Z., & Taylor, J. H. 1993, *ApJ*, 412, L33

Thorsett, S. E., Arzoumanian, Z., Camilo, F., & Lyne, A. G. 1999, *ApJ*, 523, 763

Wolszczan, A. 1994, *Science*, 264, 538

Wolszczan, A. 1996, in IAU Colloquium 160, Pulsars: Problems and Progress, ed. S. Johnston *et al.* (ASP Conf. Series Vol. 105), 91.

Table 1. Interaction cross sections

case	Normal			$e_{\text{induced}} < 0.025$		
	star ejection	planet ejection	ionization	star ejection	planet ejection	ionization
(a) 5 AU, 0.001 $M_{\odot}$	1.13±0.01	0.00±0.00	1.66±0.01	0.13±0.07	0.00±0.00	0.68±0.03
(b) 5 AU, 0.01 $M_{\odot}$	1.19±0.01	0.13±0.05	1.52±0.02	0.12±0.07	0.00±0.00	0.63±0.03
(c) 5 AU, 0.1 $M_{\odot}$	1.05±0.02	2.45±0.01	0.0000±0.00	0.14±0.07	0.79±0.03	0.00±0.00
(d) 30 AU, 0.001 $M_{\odot}$	0.007±0.004	0.000±0.000	0.008±0.004	0.001±0.001	0.000±0.000	0.003±0.001
(e) 50 AU, 0.01 $M_{\odot}$	0.001±0.001	0.000±0.000	0.003±0.002	0.0002±0.0001	0.000±0.000	0.0007±0.0002

Cross sections for the various outcomes for the cases described in §3.2. In each case, the velocity of the incoming star at infinity was  $4\text{km}\text{s}^{-1}$ .

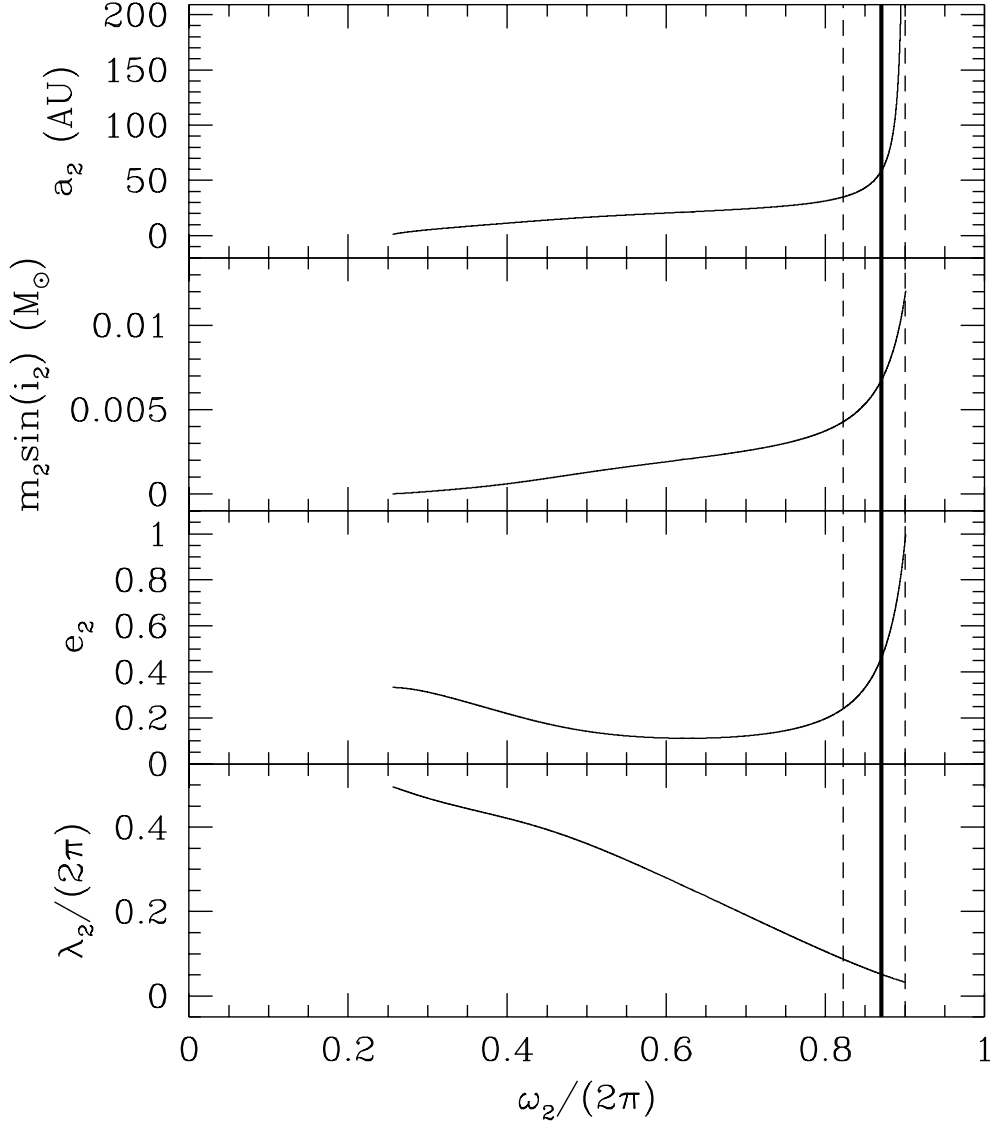


Fig. 1.— Allowed values of the semimajor axis  $a_2$ , mass  $m_2$ , eccentricity  $e_2$ , longitude at epoch  $\lambda_2$ , and longitude of pericenter  $\omega_2$  for the second companion of PSR B1620–26, using the latest available values for four pulse frequency derivatives. The vertical solid line indicates the complete solution obtained by including the preliminary value of the fifth derivative. The two dashed lines indicate the solutions obtained by decreasing the value of  $f^{(5)}$  by a factor of 1.5 (right), or increasing it by a factor of 1.5 (left).

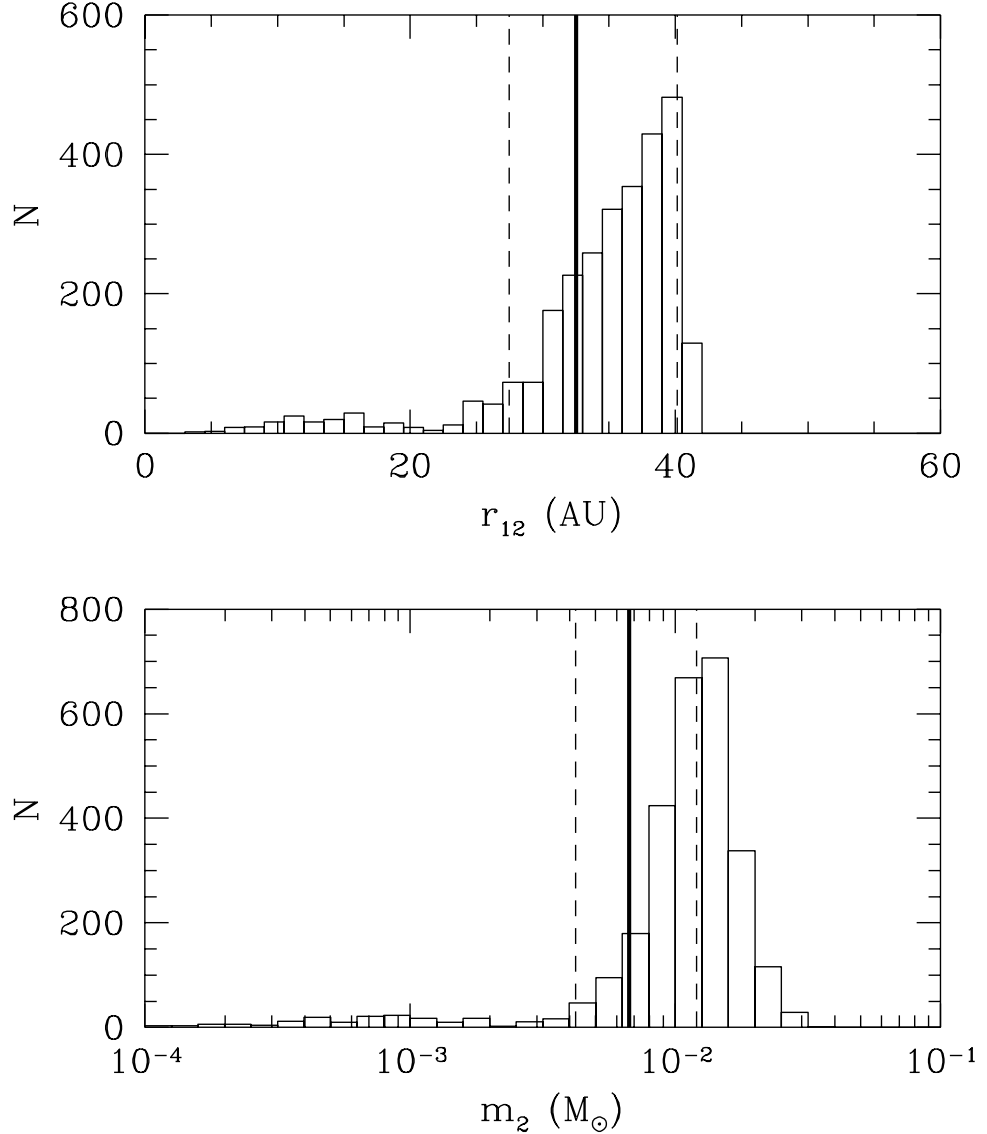


Fig. 2.— Number of accepted realizations ( $N$ ) of the triple for different values of  $m_2$  and the corresponding distance  $r_{12}$  of the second companion from the inner binary in our Monte-Carlo simulations. Accepted realizations are those leading to short-term orbital perturbation effects consistent with the current observations. The Monte-Carlo trials were performed using only the standard one-parameter family of solutions obtained from the first four pulse frequency derivatives. The solid line indicates the value given by the preliminary measurement of  $f^{(5)}$  and assuming  $\sin i_2 = 1$ . The two dashed lines indicate the values obtained by decreasing the value of  $f^{(5)}$  by a factor of 1.5 (right), or increasing it by a factor of 1.5 (left).

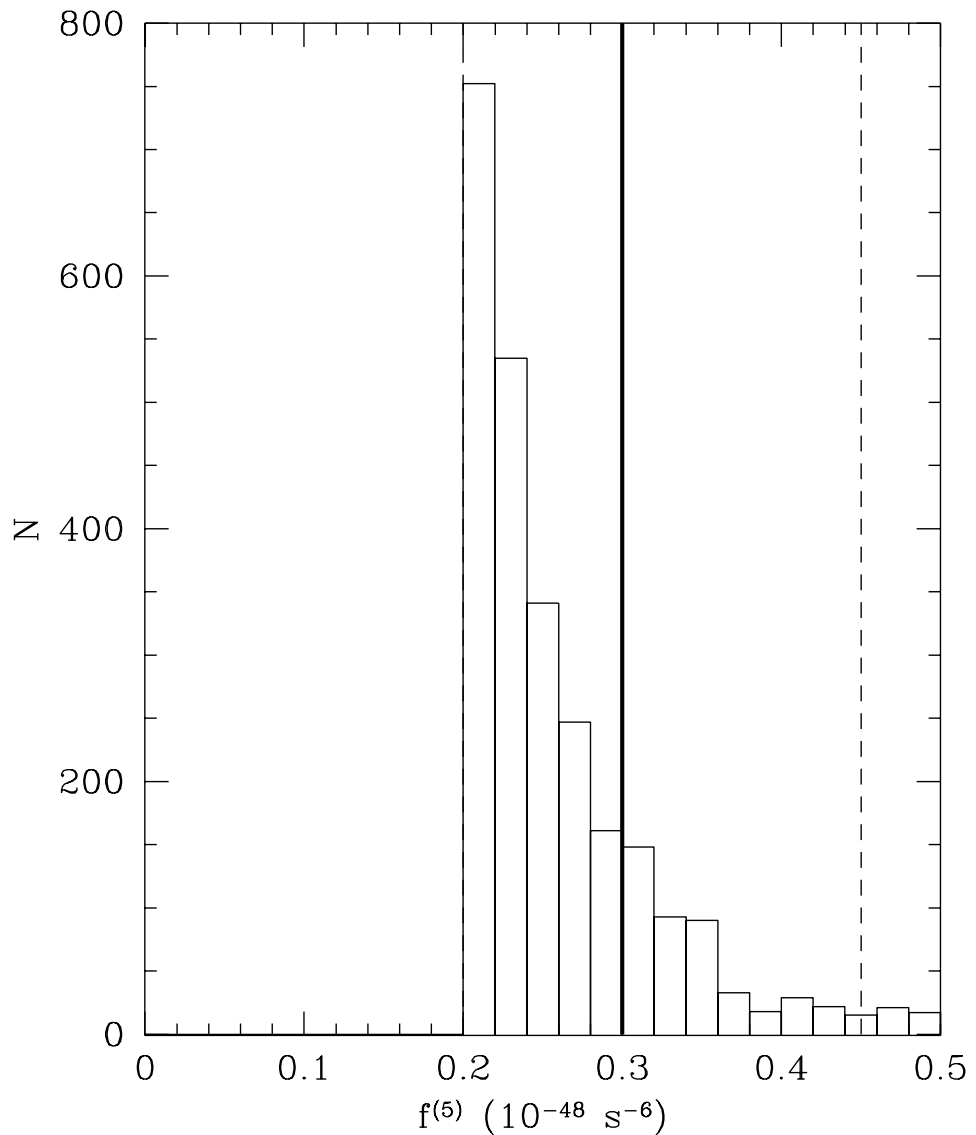


Fig. 3.— Same as Fig. 2 but for the predicted value of the fifth pulse derivative  $f^{(5)}$ . It is clear that the measured value of  $f^{(5)}$  is in perfect agreement with the theoretical expectations based on the first four derivatives and the preliminary measurements of orbital perturbation effects.

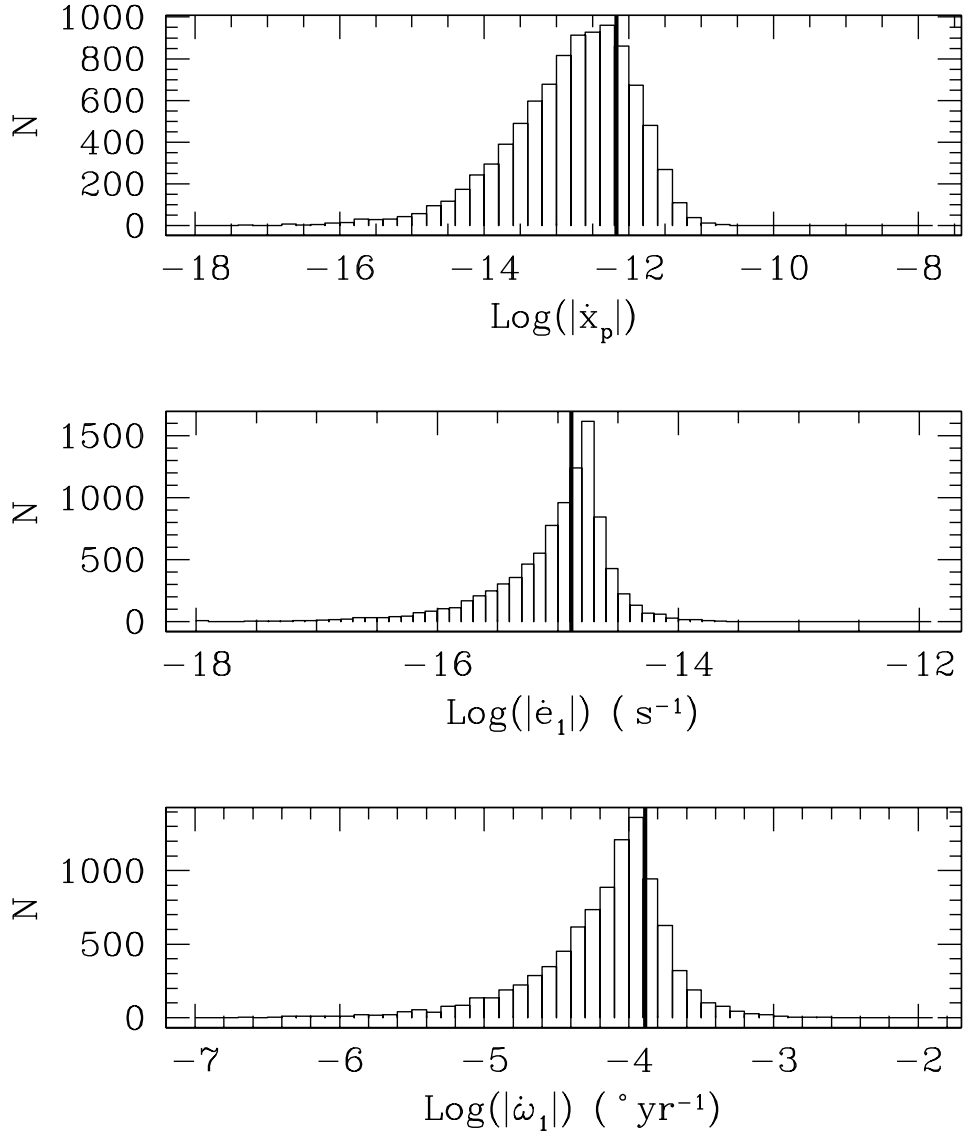


Fig. 4.— A priori probability distributions of the three secular perturbations, eqs. (2)–(4), based on the one-parameter family of solutions shown in Fig. 1 and using *only* the preliminary measurement of  $f^{(5)}$  as a constraint in the Monte-Carlo simulations. The vertical lines show the measured value (for  $\dot{x}_p$ ), or the  $1\sigma$  upper limits on the measured values (for  $\dot{e}_1$  and  $\dot{\omega}_1$ ), which are all clearly consistent with these theoretical distributions.

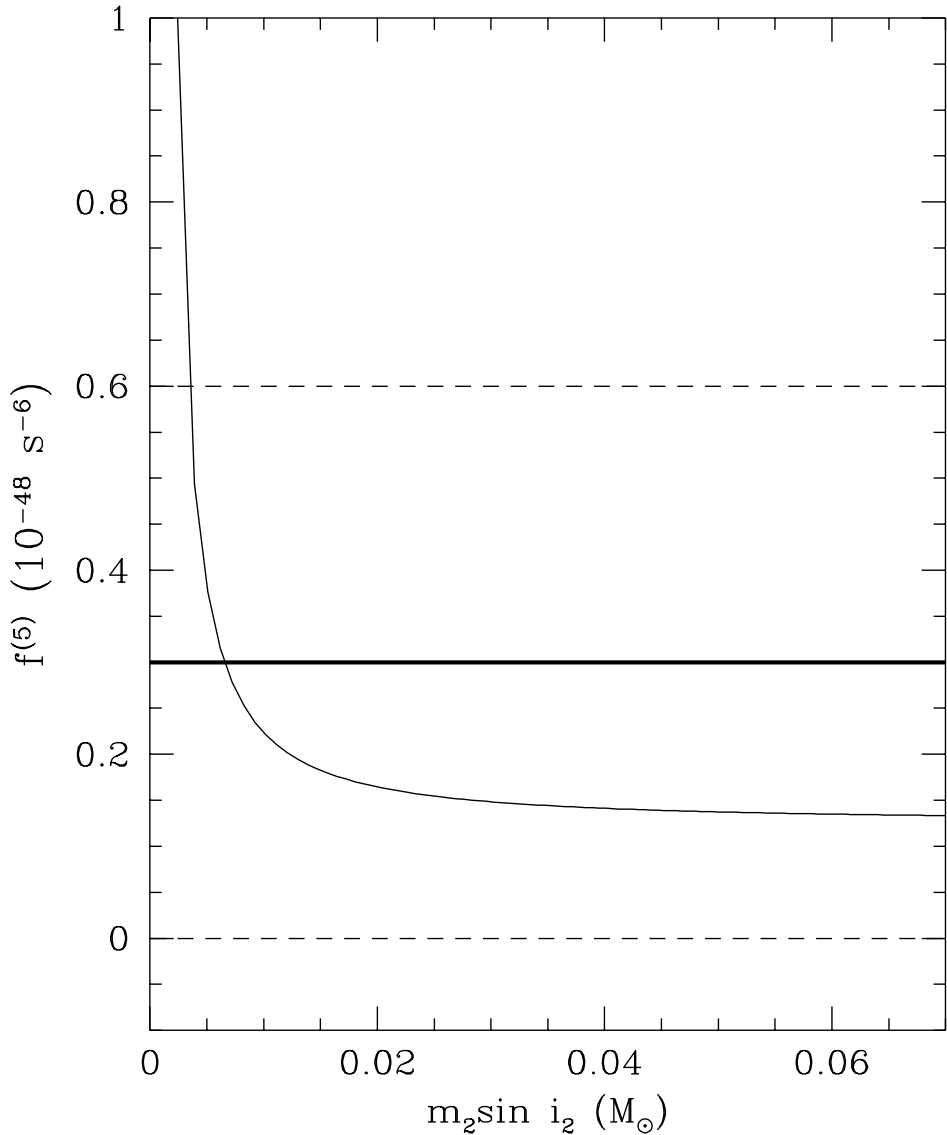


Fig. 5.— Theoretically predicted value of  $f^{(5)}$  as a function of the mass of the second companion ( $m_2$ ) for the one-parameter family of solutions based on the first four derivatives. Here we have extended these solutions into the hyperbolic regime. Values of  $m_2 \sin i_2 > 0.012 M_\odot$  correspond to a hyperbolic orbit for the second companion ( $e_2 > 1$ ). The solid horizontal line indicates the measured value of  $f^{(5)}$ , and the dashed lines correspond to the current  $1\sigma$  error. Thus the current measurement uncertainty allows all hyperbolic solutions for the second companion, and hence does not directly constrain  $m_2$ . However, for  $m_2 > 0.055 M_\odot$ , the relative velocity (“at infinity”) of the hyperbolic orbit would exceed the escape speed from the cluster core ( $\simeq 12 \text{ km s}^{-1}$ ).

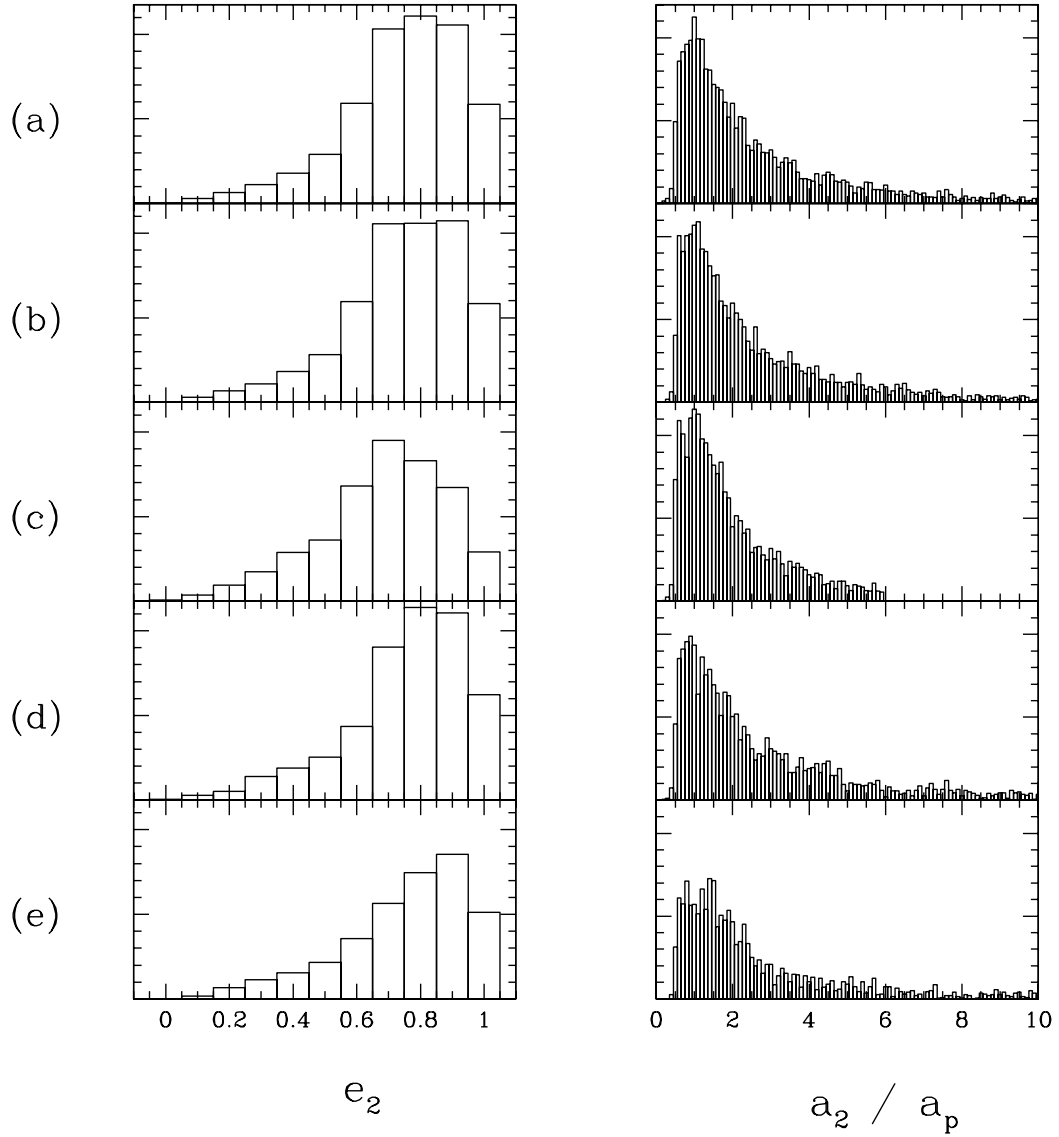


Fig. 6.— Distributions of the final eccentricity  $e_2$  and semimajor axis  $a_2$  following an exchange interaction in which a planet of mass  $m_p$  is captured by the binary pulsar. The semimajor axis is given in units of the original star–planet separation  $a_p$ . Values of  $m_p$  and  $a_p$  are (a)  $0.001 M_\odot$ , 5 AU; (b)  $0.01 M_\odot$ , 5 AU; (c)  $0.1 M_\odot$ , 5 AU; (d)  $0.001 M_\odot$ , 30 AU; (e)  $0.01 M_\odot$ , 50 AU.

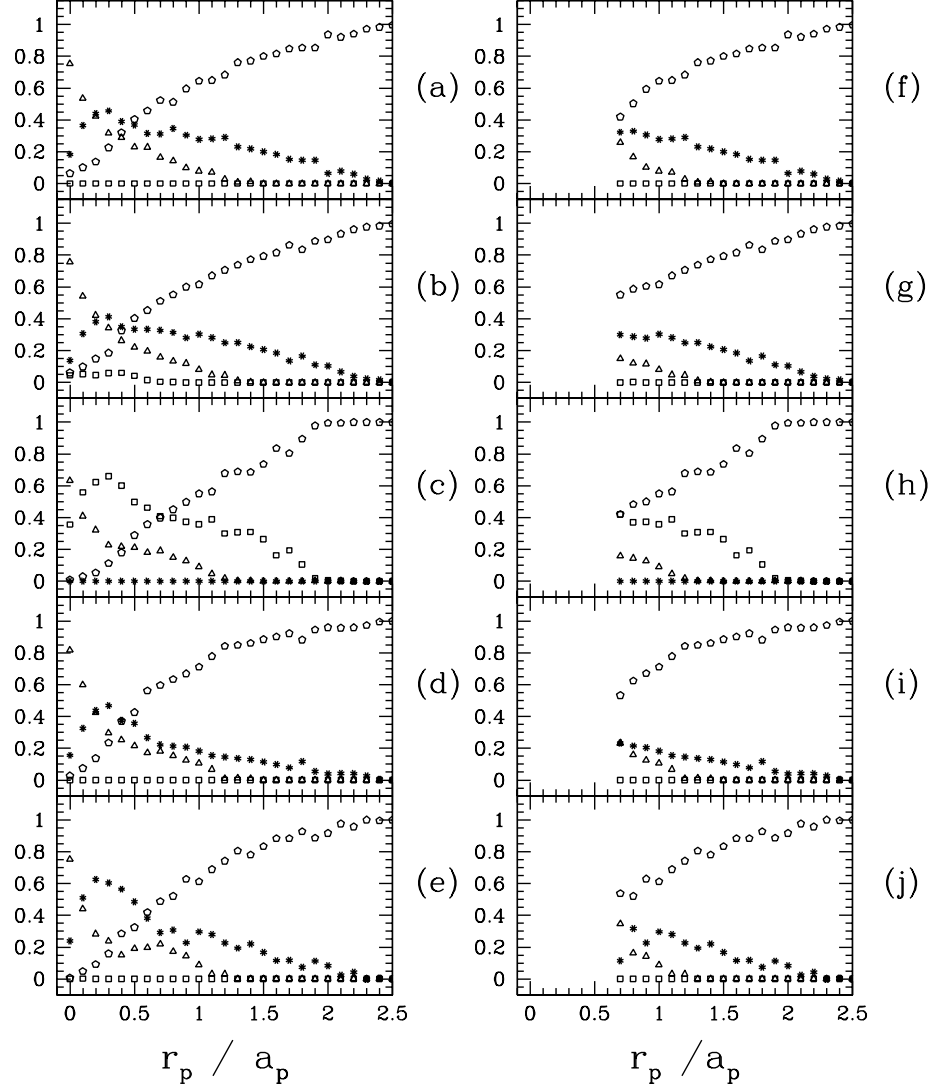


Fig. 7.— Branching ratios for various possible outcomes as a function of the distance of closest approach  $r_p$  between the binary pulsar and the main-sequence star in the parent star–planet system. The triangles represent the ejection of the star, the squares the ejection of the planet, and the pentagons a simple flyby with no exchange. Here the values of  $m_p$  and  $a_p$  are: (a,f)  $0.001 M_\odot$ , 5 AU; (b,g)  $0.01 M_\odot$ , 5 AU; (c,h)  $0.1 M_\odot$ , 5 AU; (d,i)  $0.001 M_\odot$ , 30 AU; (e,j)  $0.01 M_\odot$ , 50 AU. In panels (a)–(e) the only constraint imposed is that the binary pulsar was not disrupted during the encounter (as in Fig. 6); in panels (f)–(j) a stronger constraint was imposed, namely that the eccentricity of the binary pulsar was not perturbed to a value exceeding the presently observed value of 0.025. In all cases, we note that the branching ratio for capture of the planet remains significant, at about 10–30%.

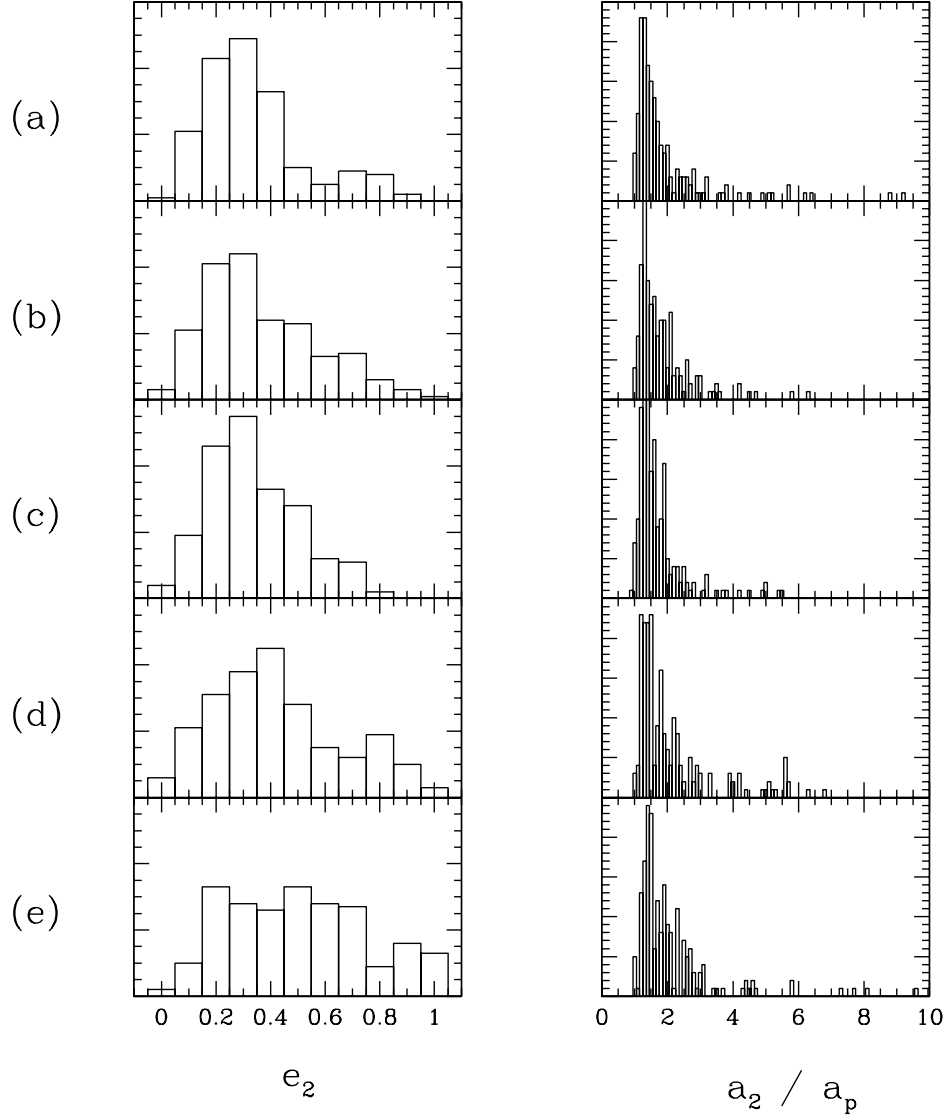


Fig. 8.— Same as Fig. 6 but with the additional constraint that the eccentricity of the binary pulsar was not perturbed to a value exceeding the presently observed value of 0.025.

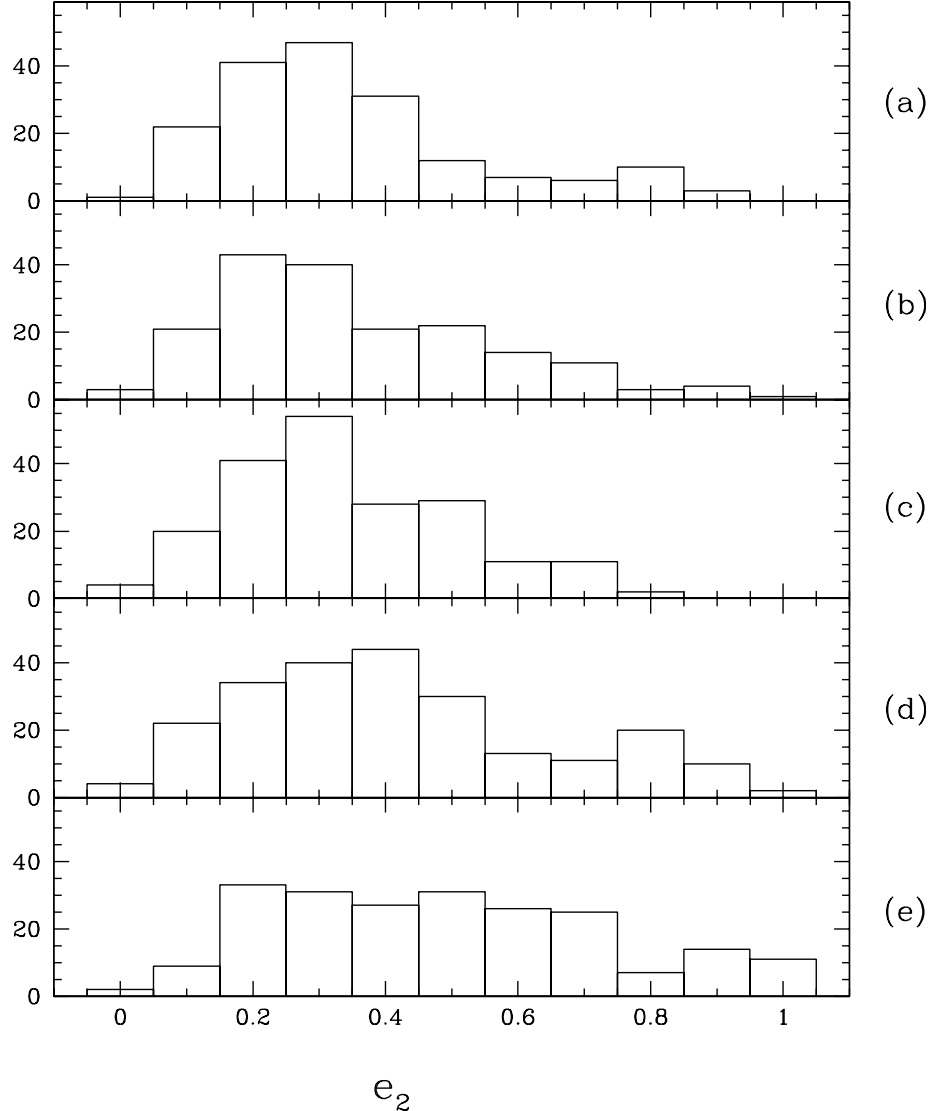


Fig. 9.— Distribution of the eccentricity induced in the binary pulsar during a dynamical exchange interaction in which a planet was captured. The panels are labeled as in Fig. 6.

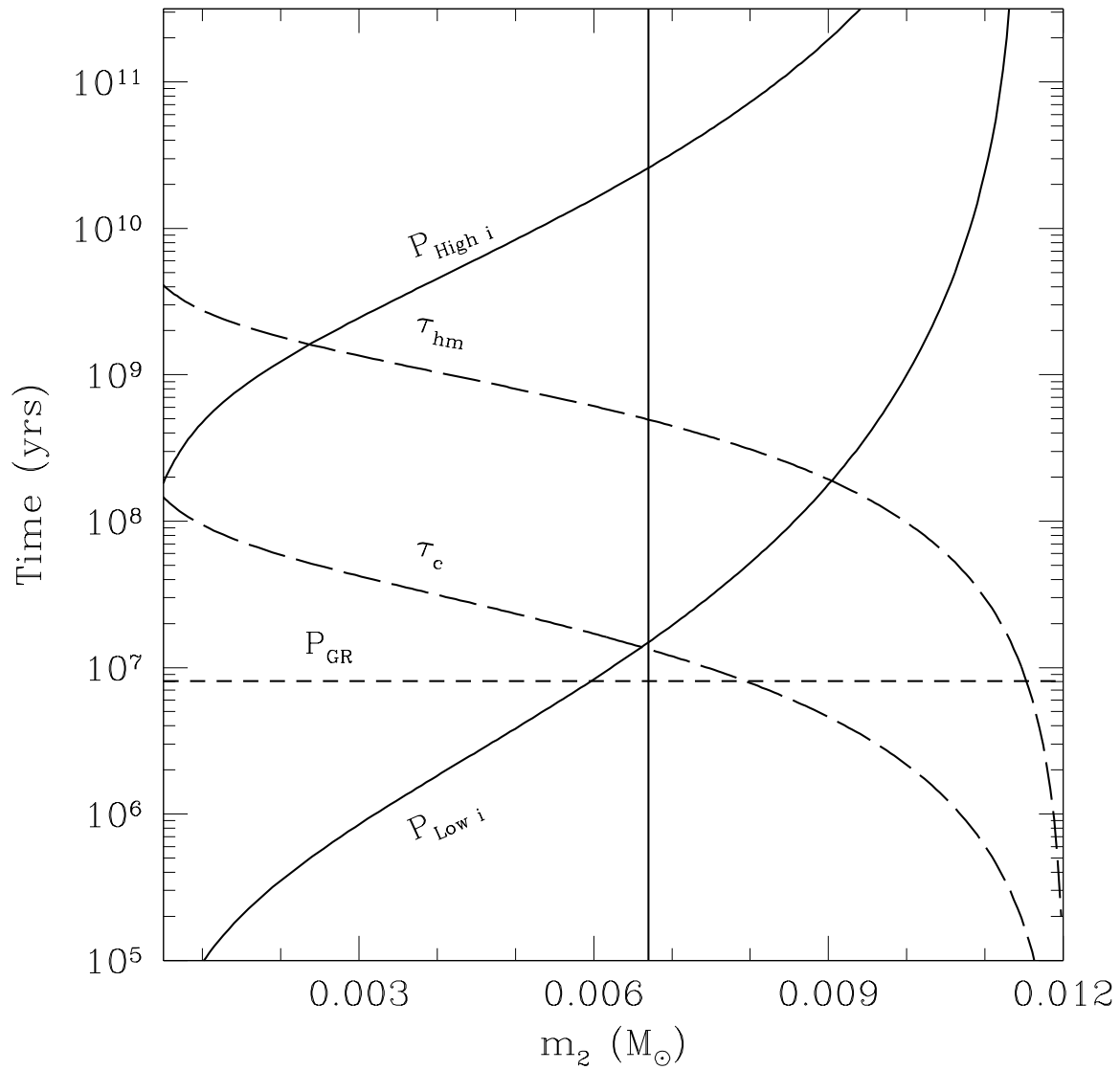


Fig. 10.— Comparison of the various secular precession timescales in the PSR B1620–26 triple, as a function of the mass of the second companion in the standard solution of §2. See text for details.

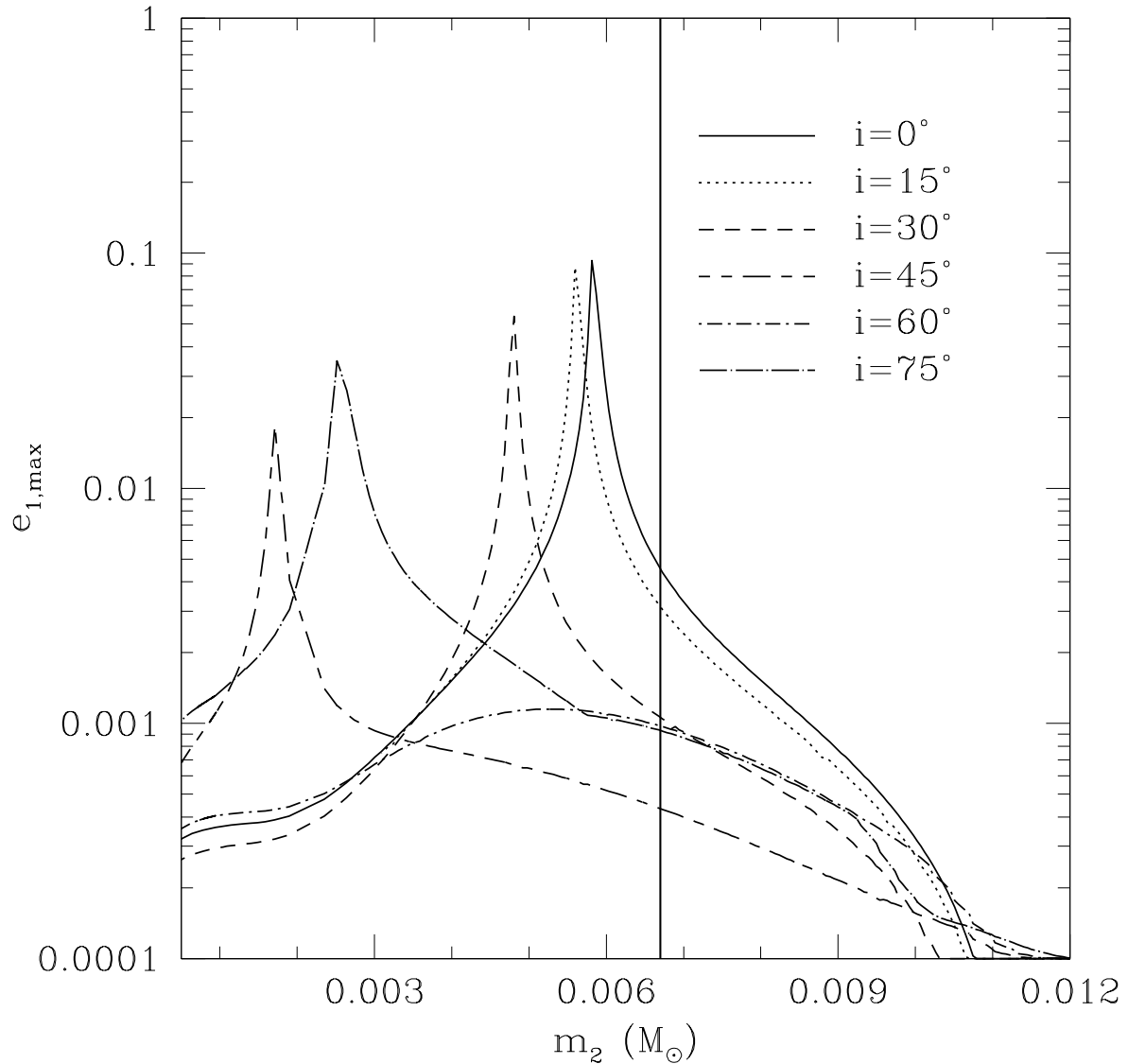


Fig. 11.— Maximum eccentricity of the binary pulsar induced by secular perturbations in the triple, as a function of the mass of the second companion in the standard solution of §2. See text for details.